Amino acids license kinase mTORC1 activity and Treg cell function via small G proteins Rag and Rheb

Hao Shi[1,*], **Nicole M. Chapman**[1,*], **Jing Wen**[1], **Cliff Guy**[1], **Lingyun Long**[1], **Yogesh Dhungana**[1], **Sherri Rankin**[1], **Stephane Pelletier**[1], **Peter Vogel**[2], **Hong Wang**[3,4], **Junmin Peng**[3,4], **Kun-Liang Guan**[5], **Hongbo Chi**[1,6,#]

[1]Department of Immunology, St. Jude Children's Research Hospital, Memphis, TN 38105, USA

[2]Department of Pathology, St. Jude Children's Research Hospital, Memphis, TN 38105, USA

[3]Department of Structural Biology and Developmental Neurobiology, St. Jude Children's Research Hospital, Memphis, TN 38105, USA

[4]Center for Proteomics and Metabolomics, St. Jude Children's Research Hospital, Memphis, TN 38105, USA

[5]Department of Pharmacology and Moores Cancer Center, University of California, San Diego, La Jolla, CA, USA

[6]Lead Contact

SUMMARY

Regulatory T (Treg) cells are critical mediators of immune tolerance whose activity depends upon T cell receptor (TCR) and mTORC1 kinase signaling, but the mechanisms that dictate functional activation of these pathways are incompletely understood. Here, we showed that amino acids license Treg cell function by priming and sustaining TCR-induced mTORC1 activity. mTORC1 activation was induced by amino acids, especially arginine and leucine, accompanied with the dynamic lysosomal localization of the mTOR and Tsc complexes. Rag and Rheb GTPases were central regulators of amino acid-dependent mTORC1 activation in effector Treg (eTreg) cells. Mice bearing RagA-RagB- or Rheb1-Rheb2-deficient Treg cells developed a fatal autoimmune disease and had reduced eTreg cell accumulation and function. RagA-RagB regulated mitochondrial and lysosomal fitness, while Rheb1-Rheb2 enforced eTreg cell suppressive gene

[#]Correspondence may be addressed to Hongbo Chi (hongbo.chi@stjude.org).

[*]These authors contributed equally

signature. Together, these findings reveal a crucial requirement of amino acid signaling for licensing and sustaining mTORC1 activation and functional programming of Treg cells.

Graphical Abstract
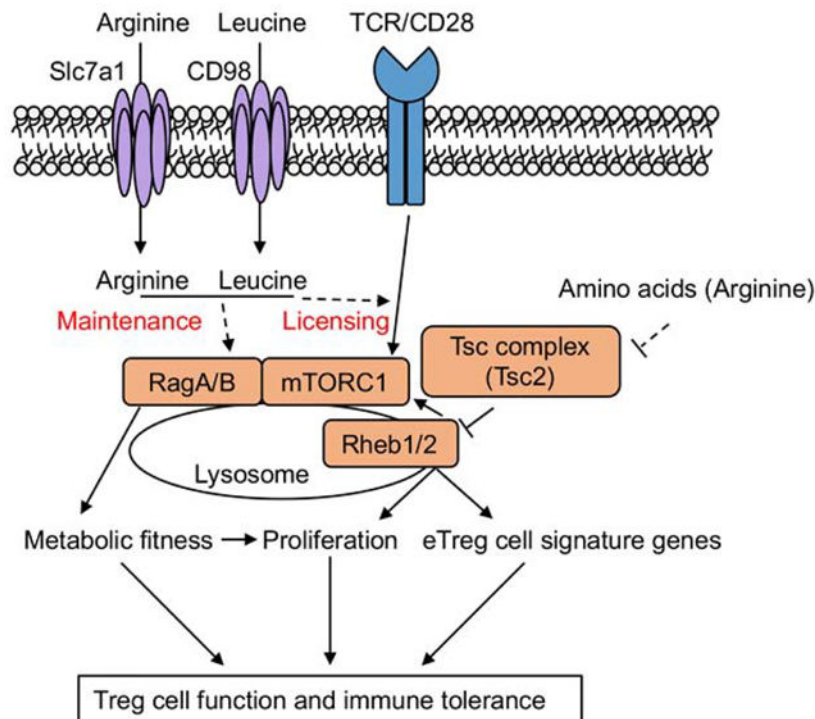
eTOC blurb

Shi and Chapman et al. show that nutrient signals from amino acids, especially arginine and leucine, are integrated by the small G proteins Rag and Rheb to orchestrate Treg cell activation and function. These data establish a crucial role for amino acid signaling in Treg cell-mediated immune suppression.

INTRODUCTION

Regulatory T (Treg) cells expressing forkhead box P3 (Foxp3) establish immune tolerance. After development, thymic-derived Treg (tTreg) cells emigrate to peripheral tissues, where T cell receptor (TCR) signals promote their conversion from $CD44^{lo}CD62L^{hi}$ central Treg (cTreg) into $CD44^{hi}CD62L^{lo}$ effector Treg (eTreg) cells (Cretney et al., 2011; Levine et al., 2014; Li and Rudensky, 2016; Smigiel et al., 2014; Vahl et al., 2014). Treg cell-specific ablation of TCRs selectively reduces eTreg cells and causes the development of systemic autoimmunity (Levine et al., 2014; Vahl et al., 2014). However, dysregulated or excessive TCR-dependent activation also disrupts eTreg cell fitness (Li and Rudensky, 2016; Wei et al., 2016). How TCR signals are propagated and tuned to impart functional eTreg cell programs remains poorly defined.

Metabolic programs and nutrient signals direct T cell activation and differentiation (Buck et al., 2017), but the roles of nutrients in Treg cells are unclear and controversial. For example, deprivation of certain amino acids promotes naïve T cell differentiation into Treg cells *in vitro* (Cobbold et al., 2009; Klysz et al., 2015; Metzler et al., 2016). However, leucine (Leu) or glutamine (Gln) deprivation or deficiency for their transporters has no effects on Treg cell differentiation *in vitro* or frequencies *in vivo* (Nakaya et al., 2014; Sinclair et al., 2013). Further, expression of Slc3a2 on Treg cells is important for their suppressive activity *in vitro*, but not for the establishment of immune tolerance *in vivo* (Ikeda et al., 2017). Whether and how amino acids can signal in Treg cells, and the functional importance *in vivo*, are currently unknown.

Treg cell responses are dependent upon mTORC1 kinase signaling (Zeng and Chi, 2017; Zeng et al., 2013), so establishing the upstream networks that tune mTORC1 activity is critical. Mammalian cell lines express amino acid sensors that activate the Rag GTPases (RagA or RagB paired with RagC or RagD) (Kim and Guan, 2019; Saxton and Sabatini, 2017). The amino acid-dependent activation of mTORC1 requires RagA *in vitro* (Kim et al., 2008; Sancak et al., 2008), but its physiological function *in vivo*, especially in the immune system, remains unclear (Efeyan et al., 2014; Kalaitzidis et al., 2017; Kim et al., 2014; Shen et al., 2016). Growth factors or amino acids also activate mTORC1 by inactivating the Tsc complex, a negative regulator of the small G protein Rheb (Carroll et al., 2016; Demetriades et al., 2014; Menon et al., 2014; Sancak et al., 2010). TCR and costimulatory signals suppress the activity of the Tsc complex (Yang et al., 2011). However, unlike deficiency of Tsc complexes that elevates mTORC1 activation (Pollizzi et al., 2015; Yang et al., 2011), TCR-induced mTORC1 activity is not completely suppressed in Rheb-deficient T cells (Yang et al., 2013). Thus, the roles of Rag and Rheb in Treg cell responses are critical to address.

Here we show that amino acid signals are integrated by Rag and Rheb family proteins to license TCR-induced mTORC1 activation in Treg cells and maintain mTORC1 signaling in eTreg cells and *in vitro*-activated Treg (aTreg) cells. We find that Treg cells require RagA and RagB (RagA/B) and Rheb1 and Rheb2 (Rheb1/2) to enforce immune homeostasis, and mice lacking these factors in Treg cells develop a *Scurfy*-like autoimmune disease. We identify a predominant role of arginine (Arg) and Leu for induction of mTORC1 activity in aTreg cells. Mechanistically, amino acids regulate the dynamics of lysosomal localization of mTOR in a RagA/B-dependent manner, as well as of the Tsc complex that antagonizes Rheb signaling, thereby pointing to the lysosome as a key signaling hub for eTreg cell function. Transcriptomics profiling and integrative analyses reveal the complementary gene expression network and cooperative roles mediated by RagA/B and Rheb1/2 for eTreg cell function and mTORC1 activation. Collectively, our results highlight that amino acid-dependent licensing of TCR-induced mTORC1 activation underlies eTreg cell-mediated immune tolerance.

RESULTS

Amino acids license TCR-dependent mTORC1 activation in Treg cells

mTORC1 activity is increased in Treg cells compared to naïve T cells (Zeng et al., 2013), but the upstream signals that promote mTORC1 activity in Treg cells remain poorly understood. Compared to naïve CD4$^+$ T cells, Treg cells had higher expression of the amino acid transporter components, CD98 and Slc7a1 (Figures 1A and 1B). Upon stimulation by amino acids, Treg cells also had a greater induction of mTORC1 activation, measured by the phosphorylation of S6 (p-S6; Figure S1A). To further elucidate the upstream mechanisms, we analyzed the relative expression of Sestrin 1 (encoded by *Sens1*; a Leu sensor) and CASTOR1 or CASTOR2 (encoded by *Gatsl3* and *Gatsl2*; Arg sensors), as well as their downstream effectors, including components in the GATOR2 complex (*Mios*) and GATOR1 complex (*Depdc5*), in naïve CD4$^+$ T cells and Treg cells (Kim and Guan, 2019; Saxton and Sabatini, 2017). Treg cells had higher expression of *Sens1, Gatsl2,* and *Gatsl3* than naïve CD4$^+$ T cells, while *Mios* and *Depdc5* were largely similar (Figure S1B). These results suggest that Treg cells are more poised for amino acid-dependent activation of mTORC1 than naïve CD4$^+$ T cells.

In selective mammalian cells, Rag GTPase activity is induced downstream of amino acids for mTORC1 activation (Kim et al., 2008; Kim and Guan, 2019; Sancak et al., 2008; Saxton and Sabatini, 2017). We therefore crossed mice carrying *lox*P-flanked RagA and RagB *(Rraga*$^{fl/fl}$*Rragb*$^{fl/fl}$*)* (Kim et al., 2014) with those expressing the *Cd4*-Cre transgene (*Cd4*^{Cre}) to delete RagA and RagB in T cells. *Cd4*^{Cre}*Rraga*$^{fl/fl}$*Rragb*$^{fl/fl}$ mice were healthy and had normal frequencies of conventional CD4$^+$ and CD8$^+$ T cells and Treg cells (see Figure S1C for gating strategy, Figure S1D) among TCRβ$^+$ T cells, which were reduced in number (Figure S1E). Also, homeostasis of CD4$^+$ T cells was largely undisturbed, while CD8$^+$ T cells showed a reduction of CD44^{hi}CD62L^{lo} effector-memory T cells (Figure S1F). We measured mTORC1 activity in Treg cells following acute amino acid starvation and restimulation with or without amino acids. Amino acid-induced p-S6 and p-4E-BP1 were largely lost in RagA/B-deficient Treg cells. Also, in the absence of amino acids, p-4E-BP1, but not p-S6, was reduced in RagA/B-deficient Treg cells (Figure 1C). To determine how Rag GTPases regulate mTORC1 activity, we generated a knock-in mouse line bearing HA-tagged RagA (HA-RagA) (Figures S1G and S1H) and performed an unbiased and quantitative interaction proteomics analysis using affinity purification coupled with mass spectrometry (AP-MS) (Shi et al., 2018). To obtain sufficient numbers of Treg cells, we generated HA-RagA-expressing Treg cells *in vitro* using anti-CD3 plus anti-CD28 (α-CD3-CD28) antibody (mAb), TGF-β and IL-2, and then immunoprecipitated the endogenous HA-RagA protein from whole cell lysates. HA-RagA interacted with the mTORC1 complex component Raptor, the Tsc complex (Tsc1, Tsc2, and Tbc1d7), amino acid sensing proteins (Sestrin 1, Sestrin 2, Sestrin 3, and CASTOR2), GATOR2 complex components (Mios, Seh1l, Wdr24, Sec13, Wdr59), and RagB, RagC, and RagD (Figure S1I). HA-RagA also co-immunoprecipitated with proteins that bind directly to the lysosome, including RAGULATOR components (Lamtor1, Lamtor2, Lamtor3, and Lamtor5) and the inside-out amino acid transporter Slc38a9 (Figure S1I). Co-immunoprecipitation followed by

immunoblot analysis validated the interaction of HA-RagA with Raptor, RagC, Lamtor2, and Tbc1d7 (Figure S1J).

These protein interaction data are consistent with RagA being localized to the lysosome, which was validated by immunofluorescence staining of HA-RagA (Figure S1K). The translocation of mTOR to the lysosome is critical for mTORC1 activation (Kim and Guan, 2019; Saxton and Sabatini, 2017). Therefore, we stimulated Foxp3-YFP$^+$ Treg cells isolated from mice that co-express YFP and Cre from the *Foxp3* locus (Chinen et al., 2016) (*Foxp3*$^{YFP-Cre/+}$, called *Foxp3*$^{Cre/+}$ for simplicity) with α-CD3-CD28 mAb overnight (hereafter called aTreg cells). We found that Foxp3-YFP$^+$ aTreg cells that were deprived of amino acids had reduced lysosomal mTOR, which was restored upon amino acid refeeding but not IL-2 stimulation (Figure 1D). RagA/B-deficient aTreg cells had a significant reduction of lysosome-associated mTOR, which was not further affected by amino acid starvation (Figure 1D). These results indicate that amino acid availability and RagA/B function regulate the dynamics of mTOR localization to the lysosome in Treg cells.

TCR stimulation induces mTORC1 activity in Treg cells (Zeng et al., 2013). To examine if amino acids affect TCR-induced mTORC1 activity, we pretreated Treg cells with amino acid-deficient or -sufficient medium, followed by α-CD3-CD28 mAb crosslinking in amino acid-deficient or -sufficient culture medium. Regardless of the initial pretreatment, Treg cells stimulated in amino acid-sufficient medium had higher mTORC1 activity than those stimulated without amino acids (Figure 1E). Moreover, RagA/B-deficient Treg cells had reduced TCR-induced activation of mTORC1 (Figure 1F), suggesting that amino acids and RagA/B signaling are prerequisites for TCR-induced mTORC1 activation. We then measured mTORC1-dependent downstream events upon TCR overnight stimulation, including the induction of cell growth and CD71 expression (Yang et al., 2013; Zeng et al., 2013). Treg cells cultured in amino acid-deficient medium did not upregulate cell size (indicated by FSC-A) or CD71 expression (Figure 1G). Similar effects were observed in RagA/B-deficient Treg cells (Figure 1H). Together, these results indicate that amino acids and RagA/B are required to license Treg cells' response to TCR stimulation necessary for mTORC1 activation.

RagA/B deficiency impairs Treg cell function

To determine the effects of RagA/B signaling on immune tolerance, we crossed *Rraga*$^{fl/fl}$*Rragb*$^{fl/fl}$ mice with *Foxp3*^{Cre} mice to delete RagA/B in Treg cells. *Foxp3*^{Cre}*Rraga*$^{fl/fl}$*Rragb*$^{fl/fl}$ mice developed a systemic inflammatory disease, indicated by enlarged secondary lymphoid organs (Figure 2A), extensive lymphocyte infiltration into the colon, liver and lung (Figure 2B), a small body size (Figure 2C), and early lethality (Figure 2D). These mice also had hyperactivation of peripheral CD4$^+$ and CD8$^+$ T cells, including elevated CD44^{hi}CD62L^{lo} effector-memory T cells (Figures 2E and S2A) and increased inflammatory cytokine production, including IFN-γ, IL-4 and IL-17 (Figures 2F, S2B and S2C). We also analyzed follicular helper T (T$_{FH}$) responses that are suppressed by Treg cells (Chung et al., 2011; Huynh et al., 2015; Linterman et al., 2011; Shrestha et al., 2015). There were a greater frequency and number of T$_{FH}$ cells and an increased frequency of germinal

center (GC) B cells in $Foxp3^{Cre}Rraga^{fl/fl}Rragb^{fl/fl}$ mice (Figures 2G and S2D). Together, RagA/B deficiency in Treg cells leads to uncontrolled inflammatory responses in mice.

To examine if RagA/B deficiency alters Treg cell suppressive molecule expression in a cell-intrinsic and inflammation-free system, we generated mixed bone marrow (BM) chimeras (see methods). RagA/B-deficient Treg cells from mixed BM chimeras had reduced expression of ICOS and CTLA4 (Figure 2H), which was also observed in $Cd4^{Cre}Rraga^{fl/fl}Rragb^{fl/fl}$ mice (Figure S2E). Similar defects in ICOS and CTLA4 expression were found in inflammation-free $Foxp3^{Cre/+}Rraga^{fl/fl}Rragb^{fl/fl}$ mice (Figure S2F; see Figures S1C and S2G for gating strategy). Additionally, RagA/B-deficient Treg cells had reduced suppressive activity *in vitro* (Figure 2I). Also, activation of Treg cells in the absence of amino acids reduced their expression of ICOS and CTLA4 and suppressive activity (Figures S2H and S2I), thus supporting a critical role for RagA/B and amino acids in Treg cell-mediated suppression and immune tolerance.

To determine the relative importance of RagA and RagB for Treg cell function, we analyzed mice with Treg cell-specific deletion of either RagA ($Foxp3^{Cre}Rraga^{fl/fl}$) or RagB ($Foxp3^{Cre}Rragb^{fl/fl}$). Both RagA-deficient and RagA/B-deficient Treg cells had reduced mTORC1 activation upon TCR stimulation, whereas RagB-deficient Treg cells displayed only a minor reduction (Figure S2J). There was an increase of the proportion of effector-memory CD4$^+$ and CD8$^+$ T cells in $Foxp3^{Cre}Rraga^{fl/fl}$ mice (Figure S2A). $Foxp3^{Cre}Rraga^{fl/fl}$ mice also had elevated IFN-γ production from conventional T cells (Figure S2B), which was similar as $Foxp3^{Cre}Rraga^{fl/fl}Rragb^{fl/fl}$ mice, while IL-4 and IL-17 were not elevated (Figure S2C). The increased frequencies of T$_{FH}$ and GC B cells were milder in $Foxp3^{Cre}Rraga^{fl/fl}$ mice than $Foxp3^{Cre}Rraga^{fl/fl}Rragb^{fl/fl}$ mice (Figures 2G and S2D). In contrast, $Foxp3^{Cre}Rragb^{fl/fl}$ mice showed no signs of T cell hyperactivation (Figures S2A–D). Therefore, RagA and RagB exhibit functional redundancy *in vivo*, with RagA playing a more dominant role than RagB.

RagA enforces eTreg cell differentiation and accumulation to control inflammation

eTreg cells are present in both lymphoid and non-lymphoid tissues, such as the lamina propria (LP) of the intestine, to mediate tissue homeostasis (Li and Rudensky, 2016). To examine cell-intrinsic effects of RagA/B deficiency and circumvent the possible effects of the inflammatory environment on Treg cell homeostasis, we analyzed mixed BM chimeras. $Foxp3^{Cre}Rraga^{fl/fl}Rragb^{fl/fl}$ chimeras had a reduction of the frequency and number of splenic eTreg cells (Figure 3A), as well as total Treg cells in the colon LP (cLP) (Figure 3B). The reduced frequency but not number of Treg cells in the cLP was evident even in the inflamed environment of $Foxp3^{Cre}Rraga^{fl/fl}Rragb^{fl/fl}$ mice (Figure 3C). We also observed a reduced frequency and number of eTreg cells in $Foxp3^{Cre/+}Rraga^{fl/fl}Rragb^{fl/fl}$ mice (Figure S3A), indicating a critical role of RagA/B in eTreg cell generation.

To determine if Rag signaling was critical for eTreg cell generation under inflammatory conditions in adult mice, we induced acute inflammation in $Foxp3^{Cre/DTR}Rraga^{fl/fl}$ mice via deletion of diphtheria toxin (DT) receptor (DTR)-expressing Treg cells ($Foxp3^{DTR}$) with DT. This treatment promotes activation and expansion of the $Foxp3^{Cre}$-expressing Treg cells to mediate immune tolerance (Chapman et al., 2018; DuPage et al., 2015). Upon DT

treatment, *Foxp3*^{Cre/DTR}*Rraga*^{fl/fl} mice, but not their respective *Foxp3*^{Cre/DTR}*Rraga*^{+/+ or +/fl} controls, developed splenomegaly and lymphadenopathy (Figure 3D). There was a decreased frequency of total Treg cells (Figure 3E) in the spleen and lymph nodes of *Foxp3*^{Cre/DTR}*Rraga*^{fl/fl} mice after DT treatment (see Figure S3B for gating strategy). The eTreg cell frequency was significantly decreased in both the spleen and lymph nodes (Figure 3F). *Foxp3*^{Cre/DTR}*Rraga*^{fl/fl} mice also had increased frequency of effector-memory CD4$^+$ T cells (Figure 3G), and increased frequencies of CD4$^+$ T cells producing IFN-γ, IL-4 and IL-17 (Figure 3H). Together, the results indicate that RagA promotes eTreg cell accumulation and Treg cell function during acute inflammation.

Arginine and leucine sustain mTORC1 activity in aTreg cells

Given the role of RagA/B in eTreg cell generation, we next examined regulation of amino acid signaling between cTreg and eTreg cells. We found that eTreg cells had increased expression of CD98 and Slc7a1 (Figure S4A). Accordingly, amino acids promoted more mTORC1 activation in eTreg than cTreg cells (Figure S4B), and Treg cells upregulated the expression of CD98 and Slc7a1 after *in vitro* TCR stimulation (Figure 4A). We next mined our previous metabolomics analysis of Treg cells (Chapman et al., 2018), which revealed increased intracellular concentrations of multiple amino acids upon activation (Figure 4B). We therefore used aTreg cells to test if amino acids maintain mTORC1 activity in the absence of continuous TCR signals. As intracellular amino acids are stored in the lysosome (Perera and Zoncu, 2016), we suppressed inside-out sensing of lysosome-derived amino acids by treatment with bafilomycin A1 (BafA1) (Abu-Remaileh et al., 2017), which inhibited mTORC1 activation in aTreg cells (Figure 4C). Further, cycloheximide (CHX) treatment, which acutely enhances intracellular concentrations of amino acids (Abu-Remaileh et al., 2017), upregulated mTORC1 activation (Figure 4D). Thus, TCR stimulation leads to intracellular amino acid accumulation and increased expression of amino acid transporters, which contribute to mTORC1 activation in aTreg cells without ongoing TCR signals.

To identify which amino acids sustain mTORC1 activation in aTreg cells, we used an unbiased, plate-based screening approach, where aTreg cells were stimulated with different combinations of amino acids. Among the single amino acids and short peptides tested (Figures S4C), Arg-containing dipeptides most strongly induced p-S6 signals (Figure 4E), suggesting an important role of Arg in promoting mTORC1 activation in aTreg cells. We also directly tested the effects of Arg by treating aTreg cells with Arg alone or in combination with other amino acids reported to increase mTORC1 activation in mammalian cells (Leu, Gln and Serine (Ser)) (Goberdhan et al., 2016). Arg treatment alone significantly induced mTORC1 activity, and the effect was much stronger than Leu or Gln. Combination of Arg and Leu or Arg, Leu and Gln further enhanced mTORC1 activity compared with Arg treatment alone (Figure 4F). Treatment with Ser alone did not alter mTORC1 activation, and Ser in combination with the above amino acids also had no additive effects (Figure S4D). These results suggest that Arg and Leu maintain mTORC1 activity in aTreg cells, consistent with the observations that Treg cells expressed Arg and Leu sensors (Figure S1B), as well as Arg and Leu transporters (Figures 1A, 1B, 4A, and S4A). Conversely, acute depletion of Arg, and to a lesser extent, Leu, but not Gln, impaired the activity of mTORC1 in aTreg cells

(Figure 4G). TCR activation of Treg cells for three days in the absence of Arg also reduced expression of ICOS and CTLA4 expression, while Leu and Gln restriction only reduced ICOS expression (Figure 4H). In mice fed Arg- or Leu-deficient diets, Treg cells had reduced expression of ICOS and CTLA4 (Figure 4I), with the number of peripheral eTreg cells modestly reduced (Figure S4E), thereby establishing the importance of Arg and Leu *in vivo*. Finally, we found that RagA/B-deficient aTreg cells were unable to activate mTORC1 in response to Arg, Gln and Leu or full amino acids (Figure 4J), and were largely insensitive to acute depletion of these amino acids (Figure S4F). The results suggest that Arg cooperates with other amino acids, especially Leu, to sustain optimal mTORC1 activation, and that RagA/B reinforce amino acid-dependent activation of mTORC1 in aTreg cells.

In addition to RagA/B, the Tsc complex can modulate mTORC1 activity downstream of either PI3K–Akt signals or amino acids (Carroll et al., 2016; Demetriades et al., 2014; Menon et al., 2014). We first examined if the inhibitory phosphorylation of Tsc2 (T1462), which is induced by TCR signals and is associated with suppression of Tsc2 GAP activity (Yang et al., 2011), was dependent on amino acids. Phosphorylation of Tsc2 in Treg cells was not affected by amino acid deficiency (Figure S4G). Next, we analyzed Tsc2 localization with the lysosome in aTreg cells upon amino acid starvation, Arg starvation, or amino acid starvation and refeeding. In the presence of amino acids, Tsc2 was dissociated from the lysosome (Figure 4K). However, deprivation of amino acids, or even Arg alone, resulted in significant enrichment of lysosomal Tsc2, whereas refeeding of amino acids led to Tsc2 dissociation from the lysosome (Figure 4K). Finally, we determined if RagA/B control the dynamics of Tsc2 with the lysosome in response to amino acids. In the presence of amino acids, Tsc2 was dissociated from the lysosome in RagA/B-deficient aTreg cells, similar as WT Treg cells. On amino acid deprivation, Tsc2 recruitment to the lysosome was only partially reduced in RagA/B-deficient aTreg cells (as compared with WT Treg cells under the same condition) (Figure S4H). Thus, amino acids orchestrate the lysosomal dissociation of the Tsc complex that is partially independent of RagA/B.

Rheb signaling regulates eTreg cell accumulation and function

Next, we explored the mechanisms downstream of Tsc2 that promote TCR and amino acid-dependent mTORC1 activation. The Tsc complex suppresses the activity of Rheb (also known as Rheb1, encoded by *Rheb*) to inhibit mTORC1 activity in cell lines (Kim and Guan, 2019; Saxton and Sabatini, 2017). However, while Tsc1- or Tsc2-deficient T cells (Pollizzi et al., 2015; Yang et al., 2011) have hyperactivation of mTORC1, Rheb can be partially or temporally dispensable for mTORC1 activity in conventional T cells (Delgoffe et al., 2009; Yang et al., 2013), which has raised concerns over the physiological significance of Tsc–Rheb signaling in T cells. We therefore generated *Foxp3*^Cre*Rheb*^fl/fl mice for Treg cell-specific deletion of *Rheb*. *Foxp3*^Cre*Rheb*^fl/fl mice appeared healthy (data not shown), in contrast to the *Scurfy*-like phenotypes of *Foxp3*^Cre*Rptor*^fl/fl mice (Zeng et al., 2013) or *Foxp3*^Cre*Rraga*^fl/fl*Rragb*^fl/fl mice described above. We did not observe alterations in the proportions of effector-memory CD4$^+$ and CD8$^+$ T cells (Figure S5A), production of inflammatory cytokines from conventional T cells (Figure S5B), or the frequency or number of Treg cells in the spleen of *Foxp3*^Cre*Rheb*^fl/fl mice (Figure S5C). As the Rheb homolog Rheb2 (encoded by *Rhebl1*) may redundantly regulate mTORC1 activation downstream of

the Tsc complex, we generated a mutant mouse line bearing germline deletion of *Rhebl1* and then bred these mice with *Foxp3*^{Cre} mice (to mark Treg cells). *Foxp3*^{Cre}*Rhebl1*$^{-/-}$ mice also showed no defects in immune homeostasis (Figures S5A–C). Therefore, unlike RagA or RagA/B, Rheb or Rheb2 is dispensable for Treg cell homeostasis and function.

Given the possible functional redundancy between Rheb and Rheb2, we next generated *Foxp3*^{Cre}*Rheb*$^{fl/fl}$*Rhebl1*$^{-/-}$ compound mutant mice, as well as *Cd4*^{Cre}*Rheb*$^{fl/fl}$*Rhebl1*$^{-/-}$ mice to dissect cell-intrinsic pathways. *Foxp3*^{Cre}*Rheb*$^{fl/fl}$*Rhebl1*$^{-/-}$ mice developed a severe and fatal inflammatory disease, resulting in small body size and signs of skin inflammation (Figure 5A, arrows), enlarged secondary lymphoid organs (Figure 5B), and early death (Figure 5C). *Foxp3*^{Cre}*Rheb*$^{fl/fl}$*Rhebl1*$^{-/-}$ mice also showed the hyperactivation of peripheral CD4$^+$ and CD8$^+$ T cells, as indicated by an accumulation of effector-memory T cells (Figure 5D) and increased inflammatory cytokine production, including IFN-γ-producing CD8$^+$ and CD4$^+$ T cells, and IL-17-producing CD4$^+$ T cells (Figure 5E). Further, *Foxp3*^{Cre}*Rheb*$^{fl/fl}$*Rhebl1*$^{-/-}$ mice had an increased frequency and number of T$_{FH}$ cells and an increased frequency but not number of GC B cells (Figure 5F). We also found that p-S6 and p-4E-BP1 were reduced in Rheb1/2-deficient Treg cells stimulated with α-CD3-CD28 mAb (Figures 5G and 5H). To test if Rheb1/2 were important for mTORC1 activation downstream of amino acids, we purified Treg cells from *Cd4*^{Cre}*Rheb*$^{fl/fl}$*Rhebl1*$^{-/-}$ mice and analyzed mTORC1 activation. In the absence of Rheb1/2, freshly-isolated Treg cells or aTreg cells had reduced induction of S6 and 4E-BP1 phosphorylation after amino acid stimulation (Figures S5D and S5E) Thus, Rheb1/2 are involved in TCR- and amino acid-inducible activation of mTORC1, and Rheb1/2 deficiency in Treg cells disrupts T cell tolerance and triggers fatal autoimmunity.

To determine if Rheb1/2, like RagA/B, mediate eTreg cell accumulation at steady state, we analyzed Treg cells from the non-inflammatory *Foxp3*$^{Cre/+}$ system. Treg cells from *Foxp3*$^{Cre/+}$*Rheb*$^{fl/fl}$*Rhebl1*$^{-/-}$ mice had a lower frequency and significantly reduced number of eTreg cells in the spleen (Figure 5I), along with a reduction of Treg cells in the cLP (Figure 5J). These defects were associated with a reduction of ICOS and CTLA4 expression (Figure 5K), which were also observed in *Cd4*^{Cre}*Rheb*$^{fl/fl}$*Rhebl1*$^{-/-}$ mice (Figure S5F). Finally, Treg cells isolated from *Cd4*^{Cre}*Rheb*$^{fl/fl}$*Rhebl1*$^{-/-}$ mice had reduced suppressive activity *in vitro* (Figure 5L). These results together show that Rheb1/2 promote mTORC1 activation, eTreg cell accumulation and Treg cell suppressive function.

RagA/B and Rheb1/2 orchestrate shared and distinct transcriptional and metabolic networks in Treg cells

To investigate the molecular mechanisms by which RagA/B and Rheb1/2 regulate eTreg cell accumulation and function, we directly compared mTORC1 activation in the two *Cd4*^{Cre}-mediated genetic models and found that, under both steady state *ex vivo* and after TCR stimulation, RagA/B- and Rheb1/2-deficient Treg cells had comparable reductions of mTORC1 activation (Figure S6A). We then stimulated WT and RagA/B- or Rheb1/2-deficient Treg cells with α-CD3-CD28 mAb for 0 or 8 h for transcriptome analysis. Gene set enrichment analysis (GSEA, FDR < 0.05) of RagA/B- and Rheb1/2-deficient Treg cells showed that the Hallmark pathways of mTORC1 signaling, Myc targets, and cholesterol

homeostasis were downregulated (Figures 6A and 6B), In addition, both RagA/B- and Rheb1/2-deficient Treg cells had defects in signatures associated with cell proliferation (Figures 6A and 6B), which was validated by FACS analysis of Ki-67 expression (Figures 6C, 6D, S6B and S6C), thus showing critical roles for RagA/B and Rheb1/2 in mTORC1 activation and proliferation that are associated with eTreg cell fitness *in vivo* (Li and Rudensky, 2016; Zeng et al., 2013).

To determine if RagA/B and Rheb1/2 orchestrate similar or discrete transcriptional signatures in Treg cells, we compared the differentially-expressed (DE) genes between RagA/B- and Rheb1/2-deficient Treg cells. Fold-change (FC) versus FC plot analysis revealed a weak positive correlation between DE genes in RagA/B- and Rheb1/2-deficient Treg cells (versus WT controls in each case) at 0 h (R = 0.29, p < 1e-4) (Figure 6E). After 8 h of stimulation, RagA/B-and Rheb1/2-deficient gene signatures were less correlated (R = 0.16, p < 1e-4) (Figure 6E), suggesting activation-induced effects on the RagA/B- and Rheb1/2-dependent transcriptional programs. We next performed functional enrichment analysis ($|\log_2 FC| > 0.5$, FDR < 0.1) in RagA/B- or Rheb1/2-deficient Treg cells (see labels Q1-Q8 in Figure 6E). Rheb1/2-deficient Treg cells primarily had decreased signatures associated with cell cycle and cellular proliferation (Figure S6D). Deficiency of RagA/B, but not Rheb1/2, reduced the expression of genes associated with nucleotide synthesis, and increased the expression of genes associated with lipid or lipoprotein metabolism (Figure S6D). Lysosome-related genes were also preferentially upregulated in activated RagA/B-deficient Treg cells (Figure S6D), and Treg cells deficient in RagA/B (Figures S6E and S6F), but not Rheb1/2 (Figure S6G), had increased lysosome content. Together, these results suggest that RagA/B and Rheb1/2 coordinately regulate Treg cell proliferation, associated with the respective control of metabolic and cell cycle programs, with only RagA/B deficiency affecting lysosome homeostasis.

We noticed that the Hallmark OXPHOS pathway and Myc targets that induce glycolytic programming in T cells (Wang et al., 2011) were downregulated in both RagA/B- and Rheb1/2-deficient Treg cells (Figures 6A and 6B). We therefore assessed mitochondrial OXPHOS (via analysis of oxygen consumption rate, OCR) and glycolysis (extracellular acidification rate, ECAR), which were reduced in RagA/B- and Rheb1/2-deficient aTreg cells (Figures 6F and 6G). As OXPHOS is mediated by mitochondrial proteins, we compared the DE genes in RagA/B- and Rheb1/2-deficient Treg cells in the MitoCarta 2.0 database (Calvo et al., 2016) (Figure 6H). We found that RagA/B-deficient Treg cells had reduced expression of a subset of mitochondria-related genes, including *Coq10b* (complex IV subunit) at steady state and *Ndufaf4* (complex I subunit) after activation, while *Mrpl47* (a mitochondrial ribosomal subunit), *Nucb2*, and *Tars* were downregulated in both contexts. Therefore, while RagA/B and Rheb1/2 are both essential for OXPHOS and glycolysis, RagA/B have more important roles than Rheb1/2 for the expression of selective mitochondrial genes.

We then analyzed mitochondrial fitness by FACS staining of TMRM (mitochondrial membrane potential), CellROX (cellular reactive oxygen species (ROS)) and Mitotracker (mitochondrial content), which were reduced in RagA/B-deficient Treg cells (Figure 6I). Imaging analysis also revealed a reduction of mitochondrial volume in RagA-deficient Treg

cells (Figure S6H). TMRM, CellROX, and Mitotracker were also reduced in Treg cells from DT-treated *Foxp3*^{Cre/DTR}*Rraga*^{fl/fl} mice (Figure S6I), further supporting a role for mitochondrial fitness downstream of RagA function in Treg cells. On the contrary, Rheb1/2-deficient Treg cells had no significant alterations of TMRM or CellROX and trended increase of Mitotracker (Figure 6J). These results collectively indicate that RagA/B have a more important role in regulating lysosomal and mitochondrial homeostasis than Rheb1/2.

RagA/B and Rheb1/2 regulate discrete eTreg cell gene signatures and signaling events

We next determined if Treg cell signature genes were differentially affected by RagA/B or Rheb1/2 deficiency. eTreg cell accumulation can decline under contexts where Foxp3 expression is reduced (DuPage et al., 2015; Wei et al., 2016). However, neither RagA/B- nor Rheb1/2-deficient Treg cells had major defects in Foxp3 expression (Figures S7A and S7B) or Foxp3-dependent gene signature (Li et al., 2014) (Figures S7C and S7D). Foxp3 expression and Treg cell identity are maintained by IL-2 signaling (Chinen et al., 2016; Shi et al., 2018). GSEA (Figures 6A and 6B) or functional enrichment analysis of DE genes (Figures 7A and S7E; see Figure 6E for Q1–Q8 designation) showed that RagA/B-deficient Treg cells had a preferential enrichment for Hallmark IL-2-STAT5 signaling, which was not observed in Rheb1/2-deficient Treg cells. This increase was likely a consequence of increased CD25 expression on RagA/B- but not Rheb1/2-deficient Treg cells (Figures 7B, 7C and S7F, S7G). Thus, neither loss of Foxp3 expression nor defective IL-2 signaling appears to account for the loss of function of RagA/B- and Rheb1/2-deficient Treg cells.

We next asked if the eTreg cell-selective program was altered in RagA/B- and Rheb1/2-deficient Treg cells. We superimposed eTreg cell signature genes (Levine et al., 2014) with DE genes in RagA/B- or Rheb1/2-deficient Treg cells (versus the WT cells) at 0 and 8 h. This analysis showed that RagA/B-deficient Treg cells had more DE eTreg cell signature genes (203 genes), but they were present in both directions, with 95 genes upregulated and 108 genes downregulated (Figure 7D). Accordingly, RagA/B-deficient Treg cells did not show significant repression of eTreg cell signatures (Figure 7D). In contrast, there were fewer DE eTreg cell signature genes overall in Rheb1/2-deficient Treg cells (109 genes). However, 77 of these eTreg cell signature genes were downregulated versus 32 upregulated, with a significant suppression for eTreg cell signatures in Rheb1/2-deficient Treg cells (Figure 7D). Thus, Rheb1/2 are more critical for inducing the expression of eTreg cell gene signature than RagA/B.

The relationship between Rag and Rheb for driving mTORC1 activity is unclear in cell lines (Sancak et al., 2010; Sancak et al., 2008). Given the above analyses and our observations that TCR-inducible mTORC1 activity was not completely ablated in either RagA/B- or Rheb1/2-deficient Treg cells (Figures 1F and 5H), we overexpressed an empty vector control or constitutively-active mutant of Rheb (Rheb Q64L) in WT or RagA/B-deficient aTreg cells, and examined their mTORC1 activity. The expression of Rheb Q64L increased mTORC1 activity in both WT and RagA/B-deficient aTreg cells, as measured by the induction of p-S6 and increase in cell size after TCR stimulation (Figures 7E and 7F), as well as elevated CD71 expression at steady state (Figure S7H). Despite the impaired mTORC1-dependent activities in RagA/B-deficient aTreg cells (versus the WT control),

Rheb Q64L had a comparable effect to upregulate mTORC1 activity in WT and RagA/B-deficient Treg cells, indicating that constitutive Rheb activation promotes mTORC1 activity even in the absence of RagA/B. Expression of Rheb Q64L also enhanced the mTORC1-dependent expression CTLA4 (Zeng et al., 2013) in both WT and RagA/B-deficient Treg cells (Figure S7I). Therefore, constitutive Rheb activity can partially overcome the requirement of RagA/B for promoting mTORC1 activity and mTORC1-dependent events in Treg cells, indicating that RagA/B and Rheb1/2 act independently, but cooperatively, to regulate mTORC1 activity in Treg cells.

DISCUSSION

Treg cells are essential for immunological tolerance, but how upstream signals regulate eTreg cell fitness remains poorly understood. In this study, we showed that the small G proteins Rag and Rheb are crucial for amino acids, especially Arg and Leu, to license and maintain TCR-dependent mTORC1 activity. The loss of RagA/B or Rheb1/2 impairs eTreg cell accumulation and function, associated with the development of fatal autoimmunity. We unveiled that RagA/B regulate metabolic programs and Rheb1/2 enforce molecular network for cell cycle progression and eTreg cell suppressive function. Thus, our studies demonstrate previously unknown roles for amino acids, RagA/B, and Rheb1/2 for licensing TCR and mTORC1 signaling in Treg cells. Costimulatory or coinhibitory signals tune specific TCR signaling pathways to drive transcriptional and metabolic programs, including mitochondrial function (Chen and Flies, 2013; Esensten et al., 2016; Klein Geltink et al., 2017). Nutrients also regulate T cell responses (Buck et al., 2017), but if and how they signal in T cells are not understood. Our findings suggest that amino acids act as a costimulatory-like signal to induce and sustain TCR-mediated mTORC1 activity via RagA/B or Rheb1/2, which enforce eTreg cell programming *in vivo*. Therefore, amino acid abundance and composition may serve as a quality control checkpoint, ensuring that sufficient nutrients are available for the induction of mTORC1-dependent anabolic programs critical for Treg cell function (Zeng and Chi, 2017; Zeng et al., 2013).

The effects and mechanisms of amino acids in Treg cells have been debatable, especially *in vivo* (Cobbold et al., 2009; Ikeda et al., 2017; Nakaya et al., 2014; Sinclair et al., 2013). We revealed that mTORC1 activity is preferentially induced and sustained by Arg and Leu in Treg cells. The selective effects of Arg and Leu were unexpected, as Gln and Ser can also promote mTORC1 activation in cell lines (Goberdhan et al., 2016; Jewell et al., 2015; Kim and Guan, 2019; Saxton and Sabatini, 2017). Amino acids, especially Arg, also promoted Tsc2 dissociation from the lysosome, a feature of amino acid signaling that has remained controversial in cell lines (Carroll et al., 2016; Demetriades et al., 2014; Menon et al., 2014). As stimulation with complete amino acids had the strongest effect on mTORC1 activation as compared with different combinations of Arg, Leu and Gln, it is possible that additional amino acids, such as isoleucine, also regulate mTORC1 activity in Treg cells (Ikeda et al., 2017). The underlying signaling mechanisms may involve alternative molecules identified in T cells or other systems (Jewell et al., 2015; Mossmann et al., 2018; Nakaya et al., 2014). How other nutrients such as cholesterol (Castellano et al., 2017) can signal to RagA/B and Rheb1/2 awaits further investigation.

Treg cell fitness and function *in vivo* are tuned by mTORC1 signaling (Zeng and Chi, 2017; Zeng et al., 2013). How extracellular cues interplay with intracellular signaling networks to shape mTORC1 activity has remained elusive. We identified Rag and Rheb as critical and functionally discrete upstream regulators of mTORC1, which likely extends to conventional T cell subsets. Indeed, despite the severe autoimmune diseases upon RagA/B and Rheb1/2 deletion in Treg cells (via *Foxp3*^Cre), we did not observe systemic autoimmune responses when deleting these molecules in all T cells (via *Cd4*^Cre), likely due to marked defects in the activation of conventional T cells in these mice (Chapman et al., 2018; Yang et al., 2013; Zeng et al., 2013). To control eTreg cell differentiation and function, RagA/B orchestrate mitochondrial fitness, which likely promotes Treg cell function and lysosomal homeostasis (Baixauli et al., 2015; Chapman et al., 2018; Weinberg et al., 2019), while Rheb1/2 induce cell cycle and eTreg cell suppressive programs. The bifurcations in downstream programs may be due to incomplete repression of mTORC1 activity in either RagA/B- or Rheb1/2-deficient Treg cells or mTORC1-independent roles for these molecules (Kalaitzidis et al., 2017; Shen et al., 2016; Tyagi et al., 2015). These differences in functional programming of Treg cells may explain why loss of Rheb1/2 led to no defects in T_H2 responses and more modest changes in T_{FH}-related responses than RagA/B deficiency. Another unexpected finding was that deletion of RagA, but not Rheb or Rheb2, alone was sufficient for disrupting immune homeostasis. The marked functional redundancy for Rheb and Rheb2 may be caused by incomplete suppression of downstream molecular targets of mTORC1, such as those regulating protein translation (Saxton and Sabatini, 2017).

In summary, our study reveals a role of amino acids as signaling molecules that license and sustain TCR-dependent mTORC1 activity in eTreg cells. The identification of Rag and Rheb downstream of amino acid signaling highlights therapeutic opportunities to target these proteins to control eTreg cell responses in autoimmune disorders and cancers (Li and Rudensky, 2016). The observations of discrete molecular networks regulated by Rag and Rheb, or the graded reductions of mTORC1 activity after deletion of RagA as compared with RagA/B, suggest that targeting of specific upstream regulators of mTORC1 may allow for tuning of selective eTreg cell functions in different diseases.

STAR Methods

LEAD CONTACT AND MATERIALS AVAILABILITY

Further information and requests for resources and reagents should be directed to and will be fulfilled by the Lead Contact, Hongbo Chi (hongbo.chi@stjude.org). Reagents, plasmids and mice generated in this study will be made available on request. A completed Materials Transfer Agreement is required for mice.

EXPERIMENTAL MODEL AND SUBJECT DETAILS

Mice—*Rheb1*^−/− and HA-RagA knock-in mice were generated in-house (see METHOD DETAILS). *Rraga*^fl/fl*Rragb*^fl/fl and *Rheb*^fl/fl mice were as described (Kim et al., 2014; Yang et al., 2013). CD45.1^+ (RRID:IMSR_JAX:002014), C57BL/6 (RRID:IMSR_JAX:000664), *Cd4*^Cre (RRID:IMSR_JAX:017336), *Foxp3*^DTR (RRID:IMSR_JAX:016958) and *Rag1*^−/− (RRID:IMSR_JAX:002216) mice were purchased from The Jackson Laboratory.

Foxp3[YFP-Cre] mice were a gift from A. Rudensky. *Foxp3*[Cre]*Rraga*^{fl/fl}*Rragb*^{fl/fl} (*Rragb*^{fl/fl} denotes male hemizygous or female homozygous mice for *Rragb* on the X-chromosome), *Foxp3*[Cre]*Rraga*^{fl/fl}, *Foxp3*[Cre]*Rragb*^{fl/fl}, *Foxp3*[Cre]*Rheb*^{fl/fl}, *Foxp3*[Cre]*Rhebl1*^{−/−} or *Foxp3*[Cre]*Rheb*^{fl/fl}*Rhebl1*^{−/−} mice and age- and gender-matched littermate controls were analyzed at the indicated ages, and both genders were used. *Cd4*[Cre]*Rraga*^{fl/fl}*Rragb*^{fl/fl} or *Cd4*[Cre]*Rheb*^{fl/fl}*Rhebl1*^{−/−} mice and littermate controls were analyzed at 6–8 weeks old. For Leu– and Arg– diet treatment condition, 6–8-week-old C57BL/6 mice that were raised on standard chow diets were fed isocaloric diets containing complete L-amino acids (control diet; A10021B) or diets deficient for L-Leu (reduced by 90%; A19050201) or L-Arg (reduced by 100%; A10036; all from Research Diets, Inc.). The composition of other nutrients, vitamins, and minerals was equivalent between these diets. After two weeks, mice were euthanized and analyzed as described (Ikeda et al., 2017). All mice were kept in a specific pathogen-free facility in the Animal Resource Center at St. Jude Children's Research Hospital. Animal protocols were approved by the Institutional Animal Care and Use Committee of St. Jude Children's Research Hospital.

Cell lines—The retroviral packaging Plat-E cells were a gift from Dr. Yun-Cai Liu, La Jolla Institute for Immunology and from female origin. The cells were cultured in Dulbecco's Modified Eagle Medium (DMEM, Thermo Fisher Scientific) supplemented with 10% fetal bovine serum (FBS) and 2 mM glutamine, 100 U/ml Penicillin and 100 μg/ml Streptomycin and maintained at 37 °C in 5% CO_2. Puromycin (1 μg/ml) and blasticidin (10 μg/ml) antibiotics were also added into the culture medium to maintain selective pressure and were removed one day before retrovirus plasmid transfection.

METHOD DETAILS

Mixed bone marrow (BM) chimeric mouse generation—To examine Treg cell homeostasis and function in a cell-intrinsic and inflammation-free system, mixed BM chimeras were generated (Karmaus et al., 2019). BM cells were extracted from femur and tibia of experimental mice (CD45.2[+]) or CD45.1[+] mice (The Jackson Laboratory). BM cells were depleted of red blood cells (RBCs) by ACK lysis buffer (Thermo Fisher Scientific), followed by depletion of T cells by a positive selection using a mixture of CD90.2, CD4 and CD8 beads (Miltenyi Biotech). 3×10^6 CD45.2[+] donor BM cells were mixed with 3×10^6 wild-type (WT) CD45.1[+] donor BM cells at a 1:1 ratio and transferred into sub-lethally irradiated (5 Gy) *Rag1*^{−/−} mice via *i.v.* injection. Analysis was performed two months later.

Analysis of *Foxp3*[Cre/DTR] mice after DT treatment—To determine if Rag signaling was critical for eTreg cell generation under inflammatory conditions in adult mice, the Foxp3[Cre/DTR] mouse model was used. *Foxp3*[Cre/DTR]*Rraga*^{fl/fl} or *Foxp3*[Cre/DTR] control mice were treated with DT (50 μg/kg) *i.p.* every other day for total four times as described (Chapman et al., 2018). Eleven days after the first injection, the mice were sacrificed. Spleen and peripheral lymph nodes were harvested and processed to form single cell suspensions for subsequent *ex vivo* FACS analysis. YFP-Foxp3^{+} and DTR-GFP^{+} signals were separated and the phenotypic analysis on Treg cells were gated on CD4^{+}TCRβ^{+}YFP^{+}GFP^{−} population.

Generation of HA-RagA mice with CRISPR-Cas9—HA-RagA knock-in mice were generated using CRISPR-Cas9 technology. Cas9 mRNA and single-guide RNA (sgRNA) were designed and generated as described previously (Pelletier et al., 2015). sgRNA targeting sites were unique in the mouse genome, with no potential off-target sites and fewer than three mismatches found using the Cas-OFFinder algorithm (Bae et al., 2014). To generate HA-RagA knock-in mice, the sequence encoding the HA epitope was inserted by co-injecting a sgRNA molecule targeting a region near the ATG of the *Rraga* gene (125 ng/μl; 5'-CTGTATTGGGCATCACCTGC), the Cas9 mRNA described above (50 ng/μl) and a single-stranded DNA molecule as a homology-directed repair (HDR) template (2 pmol/μl, 5'-CCGTTAGGCCGTGCCTCAGGCCCAGTCCGTGGCGACGCCGGCAGGTGATGTACCC ATATGATGTTCCAGATTACGCTCCCAATACAGCCATGAAGAAAAAGGTGCTGTTGA TGGGAAAGAGCGGGTC) into pronuclear-stage C57BL/6JN zygotes. Zygotes were then surgically transplanted into the oviducts of pseudo-pregnant CD1 female mice. To identify founder mice and facilitate genotyping, the sequence encoding the HA epitope also contains a NdeI restriction site (5'-CATATG-3'; see Figure S1G). Newborn mice carrying the HA-RagA knock-in allele were identified by PCR, restriction digest and Sanger sequencing using primers Rraga-N-HA_F51 (5'-AACTCGCTGTGCGCTAGATT) and Rraga-N-HA_R52 (5'-GGCGTCAGGTGAATTCTGGA). *Rhebl1*$^{-/-}$ will be described elsewhere.

FACS analysis—For analysis of surface markers, cells were stained in PBS containing 2% (w/v) bovine serum albumin on ice for 30 min, with α-CD4 (RM4-5), α-CD8α (53–6.7), α-TCRβ (H57-597), α-CD44 (1M7), α-CD62L (MEL-14), α-ICOS (398.4A), α-PD-1 (J43), α-GL7 (GL7), α-CD45.1 (A20), α-CD45.2 (104), and α-CD25 mAb (PC61.5; all from Tonbo Biosciences or Thermo Fisher Scientific); CD95 (Jo2, BD Bioscience); α-CD71 (RI7217), anti-CD98 (RL388), and α-Slc7a1 (SA191A10, BioLegend). CXCR5 was stained with biotinylated α-CXCR5 (clone 2G8) and streptavidin-conjugated PE (both from BD Biosciences) to enhance the signal. Intracellular Foxp3 (FJK-16s), CTLA4 (UC10-4B9, Biolegend), and Ki-67 (SolA15; Thermo Fisher Scientific) were analyzed in cells fixed and permeabilized with Foxp3 staining buffers per the manufacturer's instructions (Thermo Fisher Scientific). For intracellular cytokine staining, splenocytes were stimulated for 4 h with PMA and ionomycin in the presence of monensin, before intracellular staining for IFN-γ (XMG1.2), IL-4 (11B11) and IL-17 (17B7, all from Thermo Fisher Scientific) according to the manufacturer's instructions. For phosphoflow staining, cells were fixed with 1× Lyse/Fix (BD Biosciences) buffer at 37 °C for 10 min, washed and permeabilized by ice-cold Perm III buffer (BD Biosciences) on ice for 30 min, followed by staining with α-phospho-S6 (S235/236) or α-phospho-4E-BP1 (T37/46, both from Cell Signaling Technology) for 30 min at room temperature. Fixable viability dye (Thermo Fisher Scientific) was used to exclude dead cells for subsequent phosphoflow analysis. Antibody validation profiles are available via LabX (https://www.labx.com/application/antibodies-and-reagents) or CiteAb (https://www.citeab.com). FACS data were acquired on a LSRII or LSR Fortessa (BD Biosciences) and analyzed using FlowJo software (Tree Star).

Cell purification and culture—Lymphocytes were isolated from the spleen and peripheral lymph nodes (including inguinal, auxiliary and cervical lymph nodes). Treg cells

were sorted using a MoFlow (Beckman-Coulter) or Reflection (i-Cyt). CD4$^+$YFP$^+$ Treg cells were sorted from either *Foxp3*^{Cre} or *Foxp3*$^{Cre/+}$ mice and CD4$^+$CD25$^+$ Treg cells were sorted from *Cd4*^{Cre} mice. Sorted cells were cultured in plates coated with α-CD3 (2C11, 10 μg/ml) and α-CD28 (37.51, 10 μg/ml; both from Bio X Cell) for the indicated times in Click's medium (Irvine Scientific) supplemented with β-mercaptoethanol, 10% (v/v) FBS, 1% (v/v) penicillin-streptomycin and IL-2 (200 U/ml). *In vitro* Treg cell suppressive assays were performed as described (Liu et al., 2009). Briefly, WT naïve CD4$^+$CD62L$^+$CD44$^-$ T cells (constant number, 5×10^4) and Treg cells (at different ratios as indicated in the figures) were cultured in 96-well plates along with α-CD3 mAb (0.1 μg/ml) and irradiated splenocytes (constant number, 1×10^5) for 72 h, followed by thymidine incorporation assays to measure cellular proliferation. Alternatively, WT CD25$^+$ Treg cells were activated with α-CD3, α-CD28 mAb (10 μg/ml) and IL-2 (200 U/ml) for three days in amino acid-sufficient or -deficient medium (containing 10% non-dialyzed FBS), and live cells were purified by density centrifugation and used for *in vitro* suppressive assays as previously described (Zeng et al., 2013). To examine whether constitutive Rheb would rescue the RagA/B-deficient Treg cell phenotype, we overexpressed constitutive form of Rheb by retrovirus transduction. Retroviruses were produced in Plat-E cells transfected with pmCherry control or pmCherry-Rheb Q64L retroviral plasmids. For retroviral transduction, CD25$^+$ Treg cells isolated from WT or *Cd4*^{Cre}*Rraga*$^{fl/fl}$*Rragb*$^{fl/fl}$ mice were stimulated with α-CD3-CD28 mAb and IL-2 (200 U/ml) for 20 h. Transduction was performed by centrifugation as previously described (Shi et al., 2018). The cells were centrifuged 900 *g* for 3 h at room temperature in the presence of retroviral supernatants, 10 μg/ml polybrene and 200 U/ml IL-2. Treg cells were then expanded with IL-2 (200 U/ml) for 48 h. Transduced Treg cells were analyzed directly for expression of CD71 and CTLA4, or stimulated with α-CD3-CD28 mAb for 3 h in complete Click's medium before analysis of p-S6 or cell size. For Seahorse assays, Treg cells were purified from WT, *Cd4*^{Cre}*Rraga*$^{fl/fl}$*Rragb*$^{fl/fl}$ or *Cd4*^{Cre}*Rheb*$^{fl/fl}$*Rhebl1*$^{-/-}$ mice and activated for 16 h as above. Cells were washed once with Seahorse XF RPMI medium (pH 7.4, containing 5 mM glucose, 2 mM L-glutamine and 1 mM sodium pyruvate). 2×10^5 cells were seeded into one well of the 96-well seahorse assay plate. ECAR and OCR were measured under basal conditions as previously described (Du et al., 2018; Yang et al., 2017), using the Seahorse XF96 extracellular flux analyzer per the manufacturer's instructions (Agilent Tech).

Preparation of amino acid medium—To directly examine the effect of amino acid starvation and refeed on Treg cells, amino acid-deficient and -sufficient medium were made. Amino acid-free (AA−) medium was prepared using RPMI 1640 powder (R8999-04A, US Biological Life Science) and sodium phosphate dibasic (5.6 mM, the same concentration as commercially-available RPMI 1640 medium, Gibco) and supplemented with 10% (v/v) dialyzed FBS (Thermo Fisher Scientific). Amino acid-sufficient (AA+) medium was prepared by adding proper volumes of MEM amino acids solution (essential amino acids, EAA, 50×), MEM non-essential amino acids solution (NEAA, 100×) and 200 mM LGln (all from Gibco) to AA− medium to reach a final concentration of 1×EAA, 1×NEAA and 2 mM Gln. The medium was supplemented with 10% (v/v) dialyzed FBS. Medium containing single amino acid (Leu, Gln, or Arg) or their combinations was prepared with AA− medium (prepared to the same concentrations present in the AA+ medium), while medium deficient

for Leu, Gln, or Arg was prepared by adding all the essential or non-essential amino acids to AA− medium, excluding the individual amino acids (same concentration as in AA+ medium). These media were adjusted to pH 7.5, filter-sterilized (0.2 μM), and supplemented with 10% dialyzed FBS (Thermo Fisher Scientific) before use. When cells were cultured in the different amino acid-deficient medium for three days as indicated in figure legends, the medium was supplemented with 10% non-dialyzed FBS to maintain cell viability and other essential nutrients for Treg cell activation.

Short-term cell stimulation by TCR or amino acids—For short-term TCR crosslinking, sorted Treg cells were incubated in 20 μl of Click's medium containing α-CD3-biotin and α-CD28-biotin mAb (BD Biosciences, final concentrations are 5 μg/ml) on ice for 20 min and washed with 1 ml of ice-cold Click's medium. To crosslink biotinylated α-CD3-CD28 mAb, cells were incubated in Click's medium containing streptavidin (Millipore Sigma, final concentration is 5 μg/ml) on ice for 10 min. Treg cells were then activated at 37 °C for 0, 5 or 15 min. In certain assays to examine the effects of amino acids on TCR crosslinking, Treg cells were rested in either AA− or AA+ medium for 30 min at 37 °C, washed, and then stimulated as described above in either AA− or AA+ medium for 0, 5 or 15 min. For amino acid stimulation of freshly-isolated naïve CD4+ T cells and Treg cells, the cells were washed and starved in AA− medium for 30 or 60 min as indicated at 37 °C, prior to restimulation with AA− or AA+ medium for 30 min at 37 °C. For amino acid stimulation experiments with aTreg cells, freshly-isolated Treg cells were activated with α-CD3-CD28 mAb (10 μg/ml) in complete Click's medium for 18–20 h. The cells were then washed and rested in AA− medium for 1 h at 37 °C and restimulated as above. For PM-M2 plate (Biolog) screening experiments, Treg cells were isolated from IL-2/α-IL-2-complex-treated mice to generate large numbers of Treg cells (Shi et al., 2018), and activated with α-CD3-CD28 mAb for 18–20 h as described above. The aTreg cells were rested in AA− medium for 1 h, and then transferred to AA− medium (in 30 μl). The PM-M2 plate was equilibrated by adding 30 μl of AA− medium to the wells, followed by 1 h incubation at 37 °C. The 30 μl aTreg cell suspension above was then added to the wells (60 μl total volume) and incubated for 30 min. The induction of p-S6 was analyzed by phosphoflow analysis as described above.

RNA and immunoblot analysis—Real-time PCR analysis was performed with homemade primers and Sybr Green PCR Master Mix (Applied Biosystems) as described (Wei et al., 2016). Briefly, mRNAs were extracted by RNeasy Micro kit (Qiagen) from T cells, reverse transcribed from mRNA to cDNA for subsequent real-time PCR analysis. Sequences for homemade primers were as follows: *Sens1* (forward 5'-GGCCAGGACGAGGAACTTG; reverse 5'- AAGGAGTCTGCAAATAACGCAT), *Gatsl2* (forward 5'- GTCTGACCGAGACCCCTGA; reverse 5'-GACTTGGCAATCTTTGTCACAC), *Gatsl3* (forward 5'- TCGCAGTCGGTGCAAGTTC; reverse 5'- GTGAGATACGTTCATCACCAGC), *Mios* (forward 5'-ACCAAGCCCGATATTTTGTGG; reverse 5'- AAACGTAACGATCCAGCTTTGA), and *Depdc5* (forward 5'- GATGAGCTAGTCGTGAACCCT; reverse 5'-GTGAGCAATCTCCACAATGTCT). Immunoblot analysis was performed using the following antibodies as described (Shi et al., 2018): α-p-S6 (Ser235/Ser236) (2F9), α-p-4E-

BP1 (T37/46), α-p-Tsc2 (T1462) (5B12), α-Raptor (24C12), α-Lamtor2 (also called p14, D7C10), α-RagC (D8H5), α-Tsc2 (D57A9), and α-Tbc1d7 (D8K1Y, all from Cell Signaling Technology), α-HA (Bethyl Laboratories), and β-actin (AC-15; Millipore Sigma). Briefly, protein concentration in samples were quantified by BCA assay (Thermo Fisher Scientific) before loading the samples for electrophoresis and membrane transfer. The transferred membrane was blocked with TBST (0.1% Tween 20) containing 5% BSA for 1 h at room temperature before incubating with primary antibody overnight. The membrane was washed and incubated with the corresponding secondary antibody for subsequent enhanced chemiluminescent (ECL) exposure (BioRad ChemiDoc System). The band intensity of all the immunoblot was analyzed by ImageJ (NIH) software.

Immunoprecipitation and AP-MS interactome analysis—To detect the interactome of RagA protein in physiological condition, naïve CD4$^+$ T cells from C57BL/6 or HA-RagA knock-in mice were cultured in plates coated with α-CD3-CD28 mAb (10 μg/ml each) for 4.5 days in Click's medium containing IL-2 and TGF-β for differentiation into Treg cells. For immunoprecipitation, α-HA magnetic beads (Thermo Fisher Scientific) was used to pull down HA-RagA. Treg cells were lysed in IP lysis buffer (20 mM Tris-HCl pH 8.0, 137 mM NaCl, 1% Triton X-100, 2 mM EDTA) and applied to beads, incubated at 4 °C under rotation for 3 h and washed at least 3 times. Lammaeli buffer (2×) were added to each tube containing the beads and boiled for 5 min to release the bound proteins. Immunoprecipitated proteins were digested and the peptides were labeled with individual TMT reagents and pooled, followed by basic pH reversed phase LC fractionation. Each fraction was then analyzed using acidic pH reverse phase nanoscale LC-High Resolution MS/MS. Protein detection and quantification and computational analysis were performed as we described previously (Shi et al., 2018).

Immunofluorescence and histology—Foxp3-YFP$^+$ cells were sorted and cultured for 24 h in μ-slide chambered coverslips (Ibidi; 80826) coated with α-CD3-CD28 (1 μg/ml each). Cells were washed, and the medium was replaced with amino acid-sufficient and -deficient medium (as described in the text and legends). Following treatment for 30 min, cells were fixed with 2% paraformaldehyde (Electron Microscopy Sciences; 15710) for 15 min, followed by permeabilization with 0.1% Triton X-100 in PBS for 3 min. Blocking was performed in buffer comprised of PBS containing 2% bovine serum albumin and 5% donkey serum. Cells were incubated overnight at 4 °C in blocking buffer containing rat α-LAMP1 (Thermo Fisher Scientific; clone 1D4B, 1 μg/ml), rabbit α-mTOR (Cell Signaling Technology; clone 7C10, 1:250 dilution), rabbit α-Tsc2 (Cell Signaling Technology; D93F12, 1:250 dilution) or mouse α-HA mAb (Cell Signaling Technology, clone 6E2, 1:500 dilution). Cells were washed with PBS and incubated with AF647-conjugated donkey a-rat IgG (Jackson Immuno Research; catalog 712-605-153, 1 μg/ml), Cy3-conjugated donkey a-rabbit IgG (Jackson Immuno Research; catalog 711-165-152, 1 μg/ml), or Cy3-conjufated donkey a-mouse (Jackson Immuno Research; catalog 715-165-151, 1 μg/ml) and AF488-conjugated phalloidin (Thermo Fisher Scientific; catalog A12379, 1 U/ml) for 1 h at room temperature. Samples were washed with PBS, and high-resolution images were acquired using a Marianis spinning disk confocal microscope (Intelligent Imaging Innovations) equipped with a 100× 1.4NA objective, 488 nm, 561 nm and 647 nm laser lines and Prime

95B CMOS camera (Photometrics), and analyzed using Slidebook software (Intelligent Imaging Innovations). For histological analysis, tissues were fixed with 10% (v/v) neutral buffered formalin solution, embedded in paraffin, section, and stained with hematoxylin and eosin (H&E). The clinical signs of autoimmune disease or lymphocyte infiltration were analyzed by a blinded, experienced pathologist (P.V.).

QUANTIFICATION AND STATISTICAL ANALYSIS

Gene expression profiling—RNA was purified from $CD25^+$ Treg cells isolated from $Cd4^{Cre}Rraga^{fl/fl}Rragab^{fl/fl}$ or $Cd4^{Cre}Rheb^{fl/fl}Rhebl1^{-/-}$ mice or their littermate controls. Gene expression profiles were analyzed with the Affymetrix Clariom S Mouse array. The gene expression signals were summarized with the robust multi-array average algorithm implemented in R package Affycore tools v-1.50.6. Differential expression analysis was performed using R package Limma v-3.34.9 and multiple testing correction was performed using Benjamini-Hochberg methods. GSEA analysis was performed as described (Zeng et al., 2013) using the hallmark or canonical pathways (Broad Institute). DE genes ($|\log_2 FC| > 0.5$ and $FDR < 0.1$) were analyzed for functional enrichment based on the hallmark or canonical gene sets downloaded from Broad Institute using right-tailed Fisher's exact test. Gene signatures upregulated in $Foxp3^{hi}$ (GSE57272, (Li et al., 2014)) and eTreg cells (GSE61077, (Levine et al., 2014)) were defined using $|\log_2 FC| > 1$ and $FDR < 0.05$. Significance of eTreg cell signatures in RagA/B- or Rheb1/2-deficient Treg cells was calculated using Chi square test.

Statistical analysis—P values were calculated with Student's t-test, one-way ANOVA, or two-way ANOVA. $P < 0.05$ was considered significant. All error bars represent SEM.

DATA AND CODE AVAILABILITY

The microarray data of $CD4^+CD25^+$ WT and RagA/B- and Rheb1/2-deficient Treg cells from $Cd4^{Cre}$ mice have been deposited in the Gene Expression Omnibus (GEO, NCBI) under accession code GEO: GSE135739.

Supplementary Material

Refer to Web version on PubMed Central for supplementary material.

ACKNOWLEDGMENTS

REFERENCES

Abu-Remaileh M, Wyant GA, Kim C, Laqtom NN, Abbasi M, Chan SH, Freinkman E, and Sabatini DM (2017). Lysosomal metabolomics reveals V-ATPase- and mTOR-dependent regulation of amino acid efflux from lysosomes. Science 358, 807–813. [PubMed: 29074583]

Bae S, Park J, and Kim JS (2014). Cas-OFFinder: a fast and versatile algorithm that searches for potential off-target sites of Cas9 RNA-guided endonucleases. Bioinformatics 30, 1473–1475. [PubMed: 24463181]

Baixauli F, Acin-Perez R, Villarroya-Beltri C, Mazzeo C, Nunez-Andrade N, Gabande-Rodriguez E, Ledesma MD, Blazquez A, Martin MA, Falcon-Perez JM, et al. (2015). Mitochondrial Respiration Controls Lysosomal Function during Inflammatory T Cell Responses. Cell Metab 22, 485–498. [PubMed: 26299452]

Buck MD, Sowell RT, Kaech SM, and Pearce EL (2017). Metabolic Instruction of Immunity. Cell 169, 570–586. [PubMed: 28475890]

Calvo SE, Clauser KR, and Mootha VK (2016). MitoCarta2.0: an updated inventory of mammalian mitochondrial proteins. Nucleic Acids Res 44, D1251–1257. [PubMed: 26450961]

Carroll B, Maetzel D, Maddocks OD, Otten G, Ratcliff M, Smith GR, Dunlop EA, Passos JF, Davies OR, Jaenisch R, et al. (2016). Control of TSC2-Rheb signaling axis by arginine regulates mTORC1 activity. eLife 5, pii: e11058. [PubMed: 26742086]

Castellano BM, Thelen AM, Moldavski O, Feltes M, van der Welle RE, Mydock-McGrane L, Jiang X, van Eijkeren RJ, Davis OB, Louie SM, et al. (2017). Lysosomal cholesterol activates mTORC1 via an SLC38A9-Niemann-Pick C1 signaling complex. Science 355, 1306–1311. [PubMed: 28336668]

Chapman NM, Zeng H, Nguyen TM, Wang Y, Vogel P, Dhungana Y, Liu X, Neale G, Locasale JW, and Chi H (2018). mTOR coordinates transcriptional programs and mitochondrial metabolism of activated Treg subsets to protect tissue homeostasis. Nature communications 9, 2095.

Chen L, and Flies DB (2013). Molecular mechanisms of T cell co-stimulation and co-inhibition. Nature reviews. Immunology 13, 227–242.

Chinen T, Kannan AK, Levine AG, Fan X, Klein U, Zheng Y, Gasteiger G, Feng Y, Fontenot JD, and Rudensky AY (2016). An essential role for the IL-2 receptor in Treg cell function. Nat Immunol 17, 1322–1333. [PubMed: 27595233]

Chung Y, Tanaka S, Chu F, Nurieva RI, Martinez GJ, Rawal S, Wang YH, Lim H, Reynolds JM, Zhou XH, et al. (2011). Follicular regulatory T cells expressing Foxp3 and Bcl-6 suppress germinal center reactions. Nature medicine 17, 983–988.

Cobbold SP, Adams E, Farquhar CA, Nolan KF, Howie D, Lui KO, Fairchild PJ, Mellor AL, Ron D, and Waldmann H (2009). Infectious tolerance via the consumption of essential amino acids and mTOR signaling. Proceedings of the National Academy of Sciences of the United States of America 106, 12055–12060. [PubMed: 19567830]

Cretney E, Xin A, Shi W, Minnich M, Masson F, Miasari M, Belz GT, Smyth GK, Busslinger M, Nutt SL, and Kallies A (2011). The transcription factors Blimp-1 and IRF4 jointly control the differentiation and function of effector regulatory T cells. Nat Immunol 12, 304–311. [PubMed: 21378976]

Delgoffe GM, Kole TP, Zheng Y, Zarek PE, Matthews KL, Xiao B, Worley PF, Kozma SC, and Powell JD (2009). The mTOR kinase differentially regulates effector and regulatory T cell lineage commitment. Immunity 30, 832–844. [PubMed: 19538929]

Demetriades C, Doumpas N, and Teleman AA (2014). Regulation of TORC1 in response to amino acid starvation via lysosomal recruitment of TSC2. Cell 156, 786–799. [PubMed: 24529380]

Du X, Wen J, Wang Y, Karmaus PWF, Khatamian A, Tan H, Li Y, Guy C, Nguyen TM, Dhungana Y, et al. (2018). Hippo/Mst signalling couples metabolic state and immune function of CD8alpha(+) dendritic cells. Nature 558, 141–145. [PubMed: 29849151]

DuPage M, Chopra G, Quiros J, Rosenthal WL, Morar MM, Holohan D, Zhang R, Turka L, Marson A, and Bluestone JA (2015). The chromatin-modifying enzyme Ezh2 is critical for the maintenance of regulatory T cell identity after activation. Immunity 42, 227–238. [PubMed: 25680271]

Efeyan A, Schweitzer LD, Bilate AM, Chang S, Kirak O, Lamming DW, and Sabatini DM (2014). RagA, but not RagB, is essential for embryonic development and adult mice. Dev Cell 29, 321–329. [PubMed: 24768164]

Esensten JH, Helou YA, Chopra G, Weiss A, and Bluestone JA (2016). CD28 Costimulation: From Mechanism to Therapy. Immunity 44, 973–988. [PubMed: 27192564]

Goberdhan DC, Wilson C, and Harris AL (2016). Amino Acid Sensing by mTORC1: Intracellular Transporters Mark the Spot. Cell Metab 23, 580–589. [PubMed: 27076075]

Huynh A, DuPage M, Priyadharshini B, Sage PT, Quiros J, Borges CM, Townamchai N, Gerriets VA, Rathmell JC, Sharpe AH, et al. (2015). Control of PI(3) kinase in Treg cells maintains homeostasis and lineage stability. Nat Immunol 16, 188–196. [PubMed: 25559257]

Ikeda K, Kinoshita M, Kayama H, Nagamori S, Kongpracha P, Umemoto E, Okumura R, Kurakawa T, Murakami M, Mikami N, et al. (2017). Slc3a2 Mediates Branched-Chain Amino-Acid-Dependent Maintenance of Regulatory T Cells. Cell Rep 21, 1824–1838. [PubMed: 29141216]

Jewell JL, Kim YC, Russell RC, Yu FX, Park HW, Plouffe SW, Tagliabracci VS, and Guan KL (2015). Metabolism. Differential regulation of mTORC1 by leucine and glutamine. Science 347, 194–198. [PubMed: 25567907]

Kalaitzidis D, Lee D, Efeyan A, Kfoury Y, Nayyar N, Sykes DB, Mercier FE, Papazian A, Baryawno N, Victora GD, et al. (2017). Amino acid-insensitive mTORC1 regulation enables nutritional stress resilience in hematopoietic stem cells. The Journal of clinical investigation 127, 1405–1413. [PubMed: 28319048]

Karmaus PWF, Chen X, Lim SA, Herrada AA, Nguyen TM, Xu B, Dhungana Y, Rankin S, Chen W, Rosencrance C, et al. (2019). Metabolic heterogeneity underlies reciprocal fates of TH17 cell stemness and plasticity. Nature 565, 101–105. [PubMed: 30568299]

Kim E, Goraksha-Hicks P, Li L, Neufeld TP, and Guan KL (2008). Regulation of TORC1 by Rag GTPases in nutrient response. Nature cell biology 10, 935–945. [PubMed: 18604198]

Kim J, and Guan KL (2019). mTOR as a central hub of nutrient signalling and cell growth. Nature cell biology 21, 63–71. [PubMed: 30602761]

Kim YC, Park HW, Sciarretta S, Mo JS, Jewell JL, Russell RC, Wu X, Sadoshima J, and Guan KL (2014). Rag GTPases are cardioprotective by regulating lysosomal function. Nature communications 5, 4241.

Klein Geltink RI, O'Sullivan D, Corrado M, Bremser A, Buck MD, Buescher JM, Firat E, Zhu X, Niedermann G, Caputa G, et al. (2017). Mitochondrial Priming by CD28. Cell 171, 385–397 e311. [PubMed: 28919076]

Klysz D, Tai X, Robert PA, Craveiro M, Cretenet G, Oburoglu L, Mongellaz C, Floess S, Fritz V, Matias MI, et al. (2015). Glutamine-dependent alpha-ketoglutarate production regulates the balance between T helper 1 cell and regulatory T cell generation. Science signaling 8, ra97. [PubMed: 26420908]

Levine AG, Arvey A, Jin W, and Rudensky AY (2014). Continuous requirement for the TCR in regulatory T cell function. Nat Immunol 15, 1070–1078. [PubMed: 25263123]

Li MO, and Rudensky AY (2016). T cell receptor signalling in the control of regulatory T cell differentiation and function. Nature reviews. Immunology 16, 220–233.

Li X, Liang Y, LeBlanc M, Benner C, and Zheng Y (2014). Function of a Foxp3 cis-element in protecting regulatory T cell identity. Cell 158, 734–748. [PubMed: 25126782]

Linterman MA, Pierson W, Lee SK, Kallies A, Kawamoto S, Rayner TF, Srivastava M, Divekar DP, Beaton L, Hogan JJ, et al. (2011). Foxp3+ follicular regulatory T cells control the germinal center response. Nature medicine 17, 975–982.

Liu G, Burns S, Huang G, Boyd K, Proia RL, Flavell RA, and Chi H (2009). The receptor S1P1 overrides regulatory T cell-mediated immune suppression through Akt-mTOR. Nat Immunol 10, 769–777. [PubMed: 19483717]

Menon S, Dibble CC, Talbott G, Hoxhaj G, Valvezan AJ, Takahashi H, Cantley LC, and Manning BD (2014). Spatial control of the TSC complex integrates insulin and nutrient regulation of mTORC1 at the lysosome. Cell 156, 771–785. [PubMed: 24529379]

Metzler B, Gfeller P, and Guinet E (2016). Restricting Glutamine or Glutamine-Dependent Purine and Pyrimidine Syntheses Promotes Human T Cells with High FOXP3 Expression and Regulatory Properties. Journal of immunology 196, 3618–3630.

Mossmann D, Park S, and Hall MN (2018). mTOR signalling and cellular metabolism are mutual determinants in cancer. Nat Rev Cancer 18, 744–757. [PubMed: 30425336]

Nakaya M, Xiao Y, Zhou X, Chang JH, Chang M, Cheng X, Blonska M, Lin X, and Sun SC (2014). Inflammatory T cell responses rely on amino acid transporter ASCT2 facilitation of glutamine uptake and mTORC1 kinase activation. Immunity 40, 692–705. [PubMed: 24792914]

Pelletier S, Gingras S, and Green DR (2015). Mouse genome engineering via CRISPR-Cas9 for study of immune function. Immunity 42, 18–27. [PubMed: 25607456]

Perera RM, and Zoncu R (2016). The Lysosome as a Regulatory Hub. Annu Rev Cell Dev Biol 32, 223–253. [PubMed: 27501449]

Pollizzi KN, Patel CH, Sun IH, Oh MH, Waickman AT, Wen J, Delgoffe GM, and Powell JD (2015). mTORC1 and mTORC2 selectively regulate CD8(+) T cell differentiation. The Journal of clinical investigation 125, 2090–2108. [PubMed: 25893604]

Sancak Y, Bar-Peled L, Zoncu R, Markhard AL, Nada S, and Sabatini DM (2010). Ragulator-Rag complex targets mTORC1 to the lysosomal surface and is necessary for its activation by amino acids. Cell 141, 290–303. [PubMed: 20381137]

Sancak Y, Peterson TR, Shaul YD, Lindquist RA, Thoreen CC, Bar-Peled L, and Sabatini DM (2008). The Rag GTPases bind raptor and mediate amino acid signaling to mTORC1. Science 320, 1496–1501. [PubMed: 18497260]

Saxton RA, and Sabatini DM (2017). mTOR Signaling in Growth, Metabolism, and Disease. Cell 169, 361–371.

Shen K, Sidik H, and Talbot WS (2016). The Rag-Ragulator Complex Regulates Lysosome Function and Phagocytic Flux in Microglia. Cell Rep 14, 547–559. [PubMed: 26774477]

Shi H, Liu C, Tan H, Li Y, Nguyen TM, Dhungana Y, Guy C, Vogel P, Neale G, Rankin S, et al. (2018). Hippo Kinases Mst1 and Mst2 Sense and Amplify IL-2R-STAT5 Signaling in Regulatory T Cells to Establish Stable Regulatory Activity. Immunity 49, 899–914 e896. [PubMed: 30413360]

Shrestha S, Yang K, Guy C, Vogel P, Neale G, and Chi H (2015). Treg cells require the phosphatase PTEN to restrain TH1 and TFH cell responses. Nat Immunol 16, 178–187. [PubMed: 25559258]

Sinclair LV, Rolf J, Emslie E, Shi YB, Taylor PM, and Cantrell DA (2013). Control of amino-acid transport by antigen receptors coordinates the metabolic reprogramming essential for T cell differentiation. Nat Immunol 14, 500–508. [PubMed: 23525088]

Smigiel KS, Richards E, Srivastava S, Thomas KR, Dudda JC, Klonowski KD, and Campbell DJ (2014). CCR7 provides localized access to IL-2 and defines homeostatically distinct regulatory T cell subsets. The Journal of experimental medicine 211, 121–136. [PubMed: 24378538]

Tyagi R, Shahani N, Gorgen L, Ferretti M, Pryor W, Chen PY, Swarnkar S, Worley PF, Karbstein K, Snyder SH, and Subramaniam S (2015). Rheb Inhibits Protein Synthesis by Activating the PERK-eIF2alpha Signaling Cascade. Cell Rep 10, 684–693. [PubMed: 25660019]

Vahl JC, Drees C, Heger K, Heink S, Fischer JC, Nedjic J, Ohkura N, Morikawa H, Poeck H, Schallenberg S, et al. (2014). Continuous T cell receptor signals maintain a functional regulatory T cell pool. Immunity 41, 722–736. [PubMed: 25464853]

Wang R, Dillon CP, Shi LZ, Milasta S, Carter R, Finkelstein D, McCormick LL, Fitzgerald P, Chi H, Munger J, and Green DR (2011). The transcription factor Myc controls metabolic reprogramming upon T lymphocyte activation. Immunity 35, 871–882. [PubMed: 22195744]

Wei J, Long L, Yang K, Guy C, Shrestha S, Chen Z, Wu C, Vogel P, Neale G, Green DR, and Chi H (2016). Autophagy enforces functional integrity of regulatory T cells by coupling environmental cues and metabolic homeostasis. Nat Immunol 17, 277–285. [PubMed: 26808230]

Weinberg SE, Singer BD, Steinert EM, Martinez CA, Mehta MM, Martinez-Reyes I, Gao P, Helmin KA, Abdala-Valencia H, Sena LA, et al. (2019). Mitochondrial complex III is essential for suppressive function of regulatory T cells. Nature 565, 495–499. [PubMed: 30626970]

Yang K, Blanco DB, Neale G, Vogel P, Avila J, Clish CB, Wu C, Shrestha S, Rankin S, Long L, et al. (2017). Homeostatic control of metabolic and functional fitness of Treg cells by LKB1 signalling. Nature 548, 602–606. [PubMed: 28847007]

Yang K, Neale G, Green DR, He W, and Chi H (2011). The tumor suppressor Tsc1 enforces quiescence of naive T cells to promote immune homeostasis and function. Nat Immunol 12, 888–897. [PubMed: 21765414]

Yang K, Shrestha S, Zeng H, Karmaus PW, Neale G, Vogel P, Guertin DA, Lamb RF, and Chi H (2013). T cell exit from quiescence and differentiation into Th2 cells depend on Raptor-mTORC1-mediated metabolic reprogramming. Immunity 39, 1043–1056. [PubMed: 24315998]

Zeng H, and Chi H (2017). mTOR signaling in the differentiation and function of regulatory and effector T cells. Current opinion in immunology 46, 103–111. [PubMed: 28535458]

Zeng H, Yang K, Cloer C, Neale G, Vogel P, and Chi H (2013). mTORC1 couples immune signals and metabolic programming to establish T(reg)-cell function. Nature 499, 485–490. [PubMed: 23812589]

Highlights

- Amino acids license mTORC1 activation downstream of TCR and costimulatory signals.

- Arginine and leucine sustain mTORC1 activity in activated Treg cells.

- RagA-RagB drive eTreg cell accumulation and function through metabolic regulation.

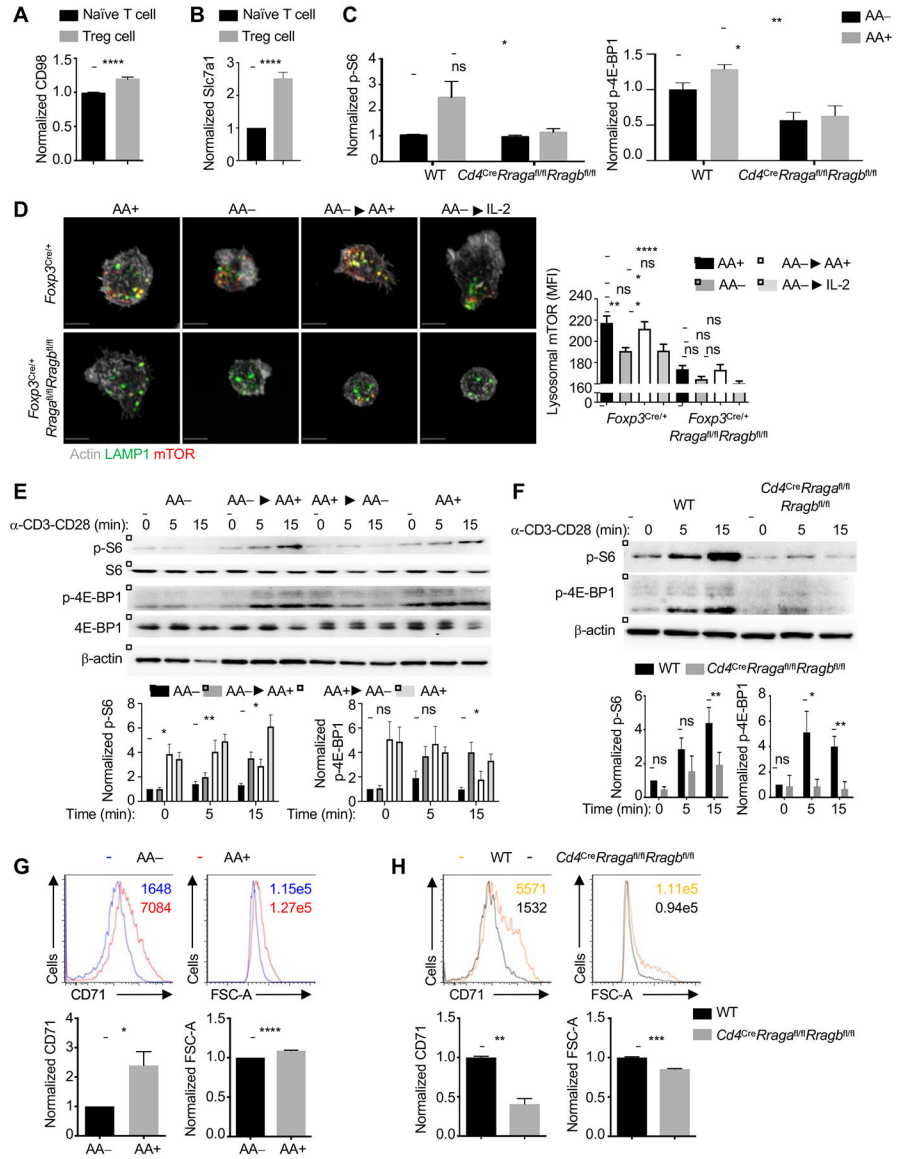- Rheb1-Rheb2 promote cell cycle and suppressive gene signature of eTreg cells.

Figure 1. Amino acids and RagA/B signaling license TCR-inducible mTORC1 activity

(A and B) CD98 (A; n = 8) or Slc7a1 (B; n = 4) expression on naïve CD4^{+} T cells and Foxp3^{+} Treg cells. (C) Quantification of phosphorylated S6 (p-S6) or p-4E-BP1 (n = 3) in Treg cells from WT or $Cd4^{Cre}Rraga^{fl/fl}Rragb^{fl/fl}$ mice stimulated with amino acid-deficient (AA−) or amino acid-sufficient (AA+) medium. (D) Imaging analysis of mTOR localization with lysosome in WT or RagA/B-deficient aTreg cells (isolated from the indicated mice and stimulated overnight with α-CD3-CD28 mAb and IL-2) under the selective conditions. Right, quantification of lysosomal mTOR in WT or RagA/B-deficient aTreg cells (> 30 cells per condition from 2 biological replicates). Scale bar: 5 μm. (E) Immunoblot analysis of phosphorylated and total S6 and 4E-BP1 in Treg cells pretreated with or without amino acids, followed by α-CD3-CD28 mAb crosslinking in the presence or absence of amino acids. Bottom, quantification of p-S6 and p-4E-BP1 normalized to β-actin (n = 6). (F) Immunoblot analysis of p-S6 and p-4E-BP1 in Treg cells from WT or

Cd4^{Cre}*Rraga*$^{fl/fl}$*Rragb*$^{fl/fl}$ mice after stimulation with α-CD3-CD28 mAb crosslinking. Bottom, quantification of p-S6 and p-4E-BP1 normalized to β-actin (n > 2). (G) CD71 expression and cell size (FSC-A) in Treg cells stimulated with α-CD3-CD28 mAb overnight in the presence or absence of amino acids. Bottom, quantification of CD71 expression and FSC-A (n = 5). (H) Treg cells from WT or *Cd4*^{Cre}*Rraga*$^{fl/fl}$*Rragb*$^{fl/fl}$ mice were stimulated with α-CD3-CD28 mAb overnight for analysis of CD71 expression and cell size. Bottom, quantification of CD71 expression and FSC-A (n = 3). Numbers in histograms show the mean fluorescence intensity. Data in graphs represent mean ± SEM. ns, not significant; *p < 0.05; **p < 0.01; ***p < 0.001; ****p < 0.0001; two-tailed Student's t-test (A, B, F, G, H), one-way ANOVA (C, D), or two-way ANOVA (E). Data are representative of one (H), two (D, RagA/B-deficient Treg cells; F, 5 min timepoint), three (D, WT Treg cells), five (F, RagA/B-deficient Treg cells at 0 or 15 min; H) or six (E, F, WT Treg cells at 0 or 15 min), or pooled from two (A–C, F, 5 min timepoint) or three (E, F, 0 and 15 min timepoints; G) independent experiments. See also Figure S1.
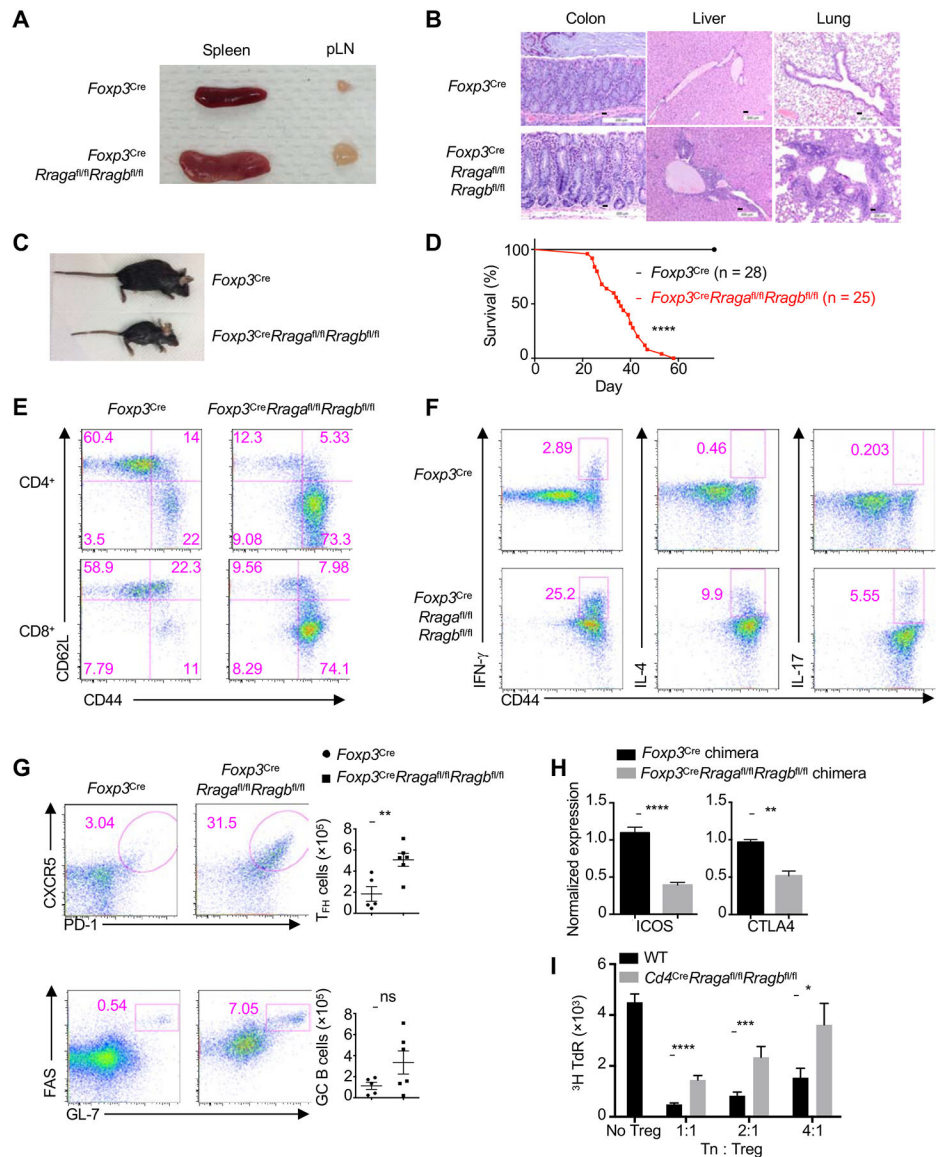
Figure 2. Development of fatal autoimmunity upon Treg cell-specific deletion of RagA/B
(A) Representative image of the spleen and peripheral lymph nodes (pLN) from 1.5-month-old *Foxp3*^{Cre} or *Foxp3*^{Cre}*Rraga*$^{fl/fl}$*Rragb*$^{fl/fl}$ mice. (B) H&E staining of the colon, liver and lung of *Foxp3*^{Cre} or *Foxp3*^{Cre}*Rraga*$^{fl/fl}$*Rragb*$^{fl/fl}$ mice. Scale bar: 200 μm. (C) Image of *Foxp3*^{Cre} or *Foxp3*^{Cre}*Rraga*$^{fl/fl}$*Rragb*$^{fl/fl}$ mice. (D) Survival of *Foxp3*^{Cre} or *Foxp3*^{Cre}*Rraga*$^{fl/fl}$*Rragb*$^{fl/fl}$ mice. (E) FACS analysis of CD44 and CD62L expression on splenic CD4$^+$Foxp3$^-$ (depicted as CD4$^+$) and CD8$^+$ T cells from *Foxp3*^{Cre} or *Foxp3*^{Cre}*Rraga*$^{fl/fl}$*Rragb*$^{fl/fl}$ mice. (F) FACS analysis of IFN-γ, IL-4, and IL-17 expression in splenic CD4$^+$Foxp3$^-$ cells from *Foxp3*^{Cre} or *Foxp3*^{Cre}*Rraga*$^{fl/fl}$*Rragb*$^{fl/fl}$ mice. (G) FACS analysis of PD-1$^+$CXCR5$^+$ T cells (top) and GL-7$^+$FAS$^+$FH GC B cells (bottom). Right, Quantification of T$_{FH}$ cell and GC B cell numbers (n ≥ 5). (H) Quantification of ICOS and CTLA4 expression in CD45.2$^+$YFP$^+$ Treg cells from *Foxp3*^{Cre} or *Foxp3*^{Cre}*Rraga*$^{fl/fl}$*Rragb*$^{fl/fl}$ mixed BM chimeras (n = 3 for CTLA4; n = 7 for ICOS). (I)

Suppressive activity of Treg cells from WT or $Cd4^{Cre}Rraga^{fl/fl}Rragb^{fl/fl}$ mice (n = 3). Numbers on plots are the frequency of cells in indicated gates. Data in graphs represent mean ± SEM. ns, not significant; *p < 0.05; **p < 0.01; ***p < 0.001; ****p < 0.0001; two-tailed Student's t-test. Data are representative of two (B) or three (A, C, E–G, I), or pooled from two (H) or four (G) independent experiments. See also Figure S2.
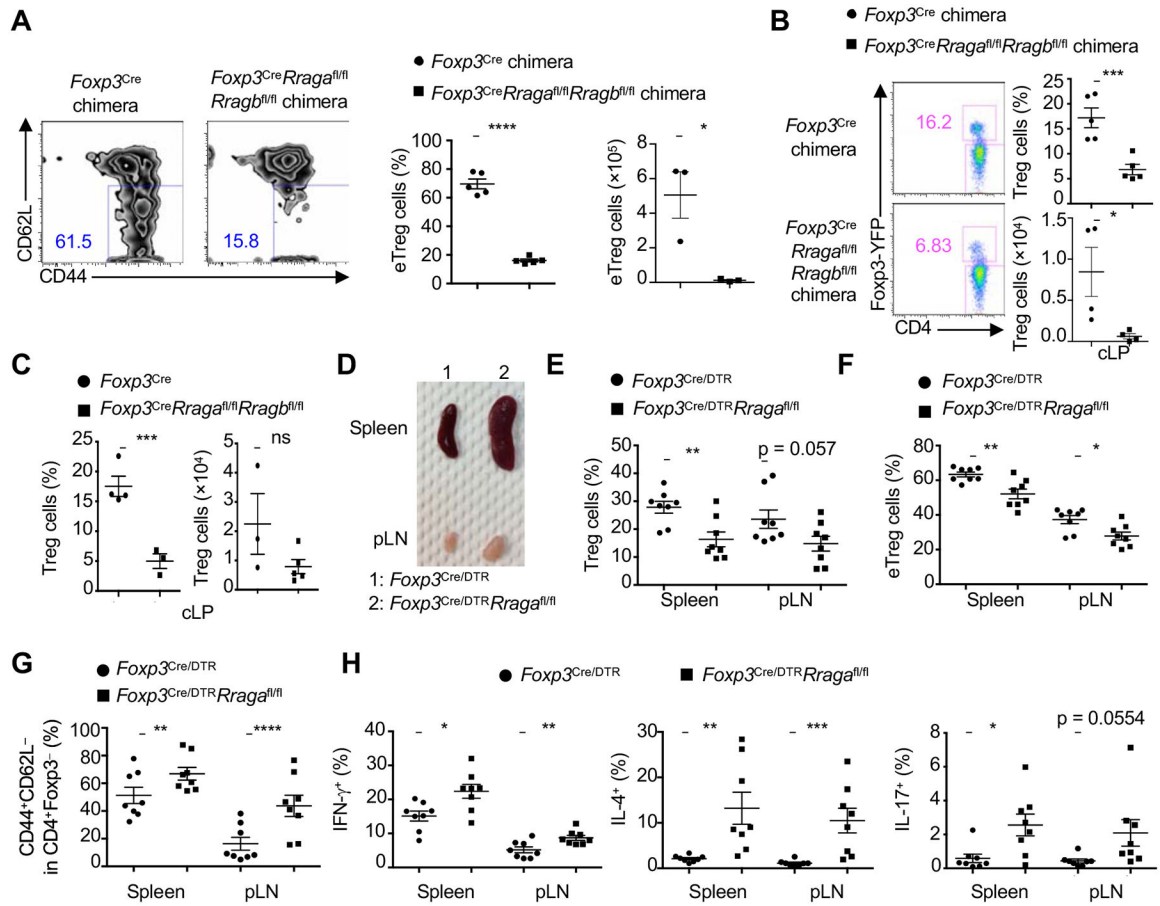
Figure 3. RagA promotes eTreg cell accumulation and function

(A) FACS analysis of CD44 and CD62L expression on CD45.2$^+$ Foxp3-YFP$^+$ Treg cells from *Foxp3*^{Cre} or *Foxp3*^{Cre}*Rraga*$^{fl/fl}$*Rragb*$^{fl/fl}$ mixed BM chimeras. Right, quantification of frequency and number of CD44^{hi}CD62L^{lo} eTreg cells in the spleen (n   3). (B) FACS analysis of Foxp3-YFP$^+$ Treg cells in the colon lamina propria (cLP) of *Foxp3*^{Cre} or *Foxp3*^{Cre}*Rraga*$^{fl/fl}$*Rragb*$^{fl/fl}$ chimeras. Right, quantification of the frequency and number of Treg cells in the cLP (n   4). (C) Quantification of the frequency and number of Treg cells in the cLP of *Foxp3*^{Cre} or *Foxp3*^{Cre}*Rraga*$^{fl/fl}$*Rragb*$^{fl/fl}$ mice (n   3). (D–H) *Foxp3*$^{Cre/DTR}$ or *Foxp3*$^{Cre/DTR}$*Rraga*$^{fl/fl}$ mice were treated with diphtheria toxin (DT). (D) Image of spleen and peripheral lymph nodes (pLN). (E) Quantification of splenic Foxp3-YFP$^+$ Treg cell frequency (n = 8). (F) Quantification of CD44^{hi}CD62L^{lo}Foxp3-YFP$^+$ eTreg cell frequency (n = 8). (G) Quantification of CD44$^+$CD62L$^-$ CD4$^+$Foxp3$^-$ T cell frequency in the spleen and pLN (n = 8). (H) Quantification of the frequencies of IFN-γ $^+$, IL-4$^+$, and IL-17$^+$ CD4$^+$Foxp3$^-$ T cells (n = 8). Numbers on plots are the frequency of cells in indicated gates. Data in graphs represent mean ± SEM. ns, not significant; *p < 0.05; **p < 0.01; ***p < 0.001; ****p < 0.0001; two-tailed Student's t-test. Data are representative of four (D), or pooled from three (C) or four (A, B, E–H) independent experiments. See also Figure S3.
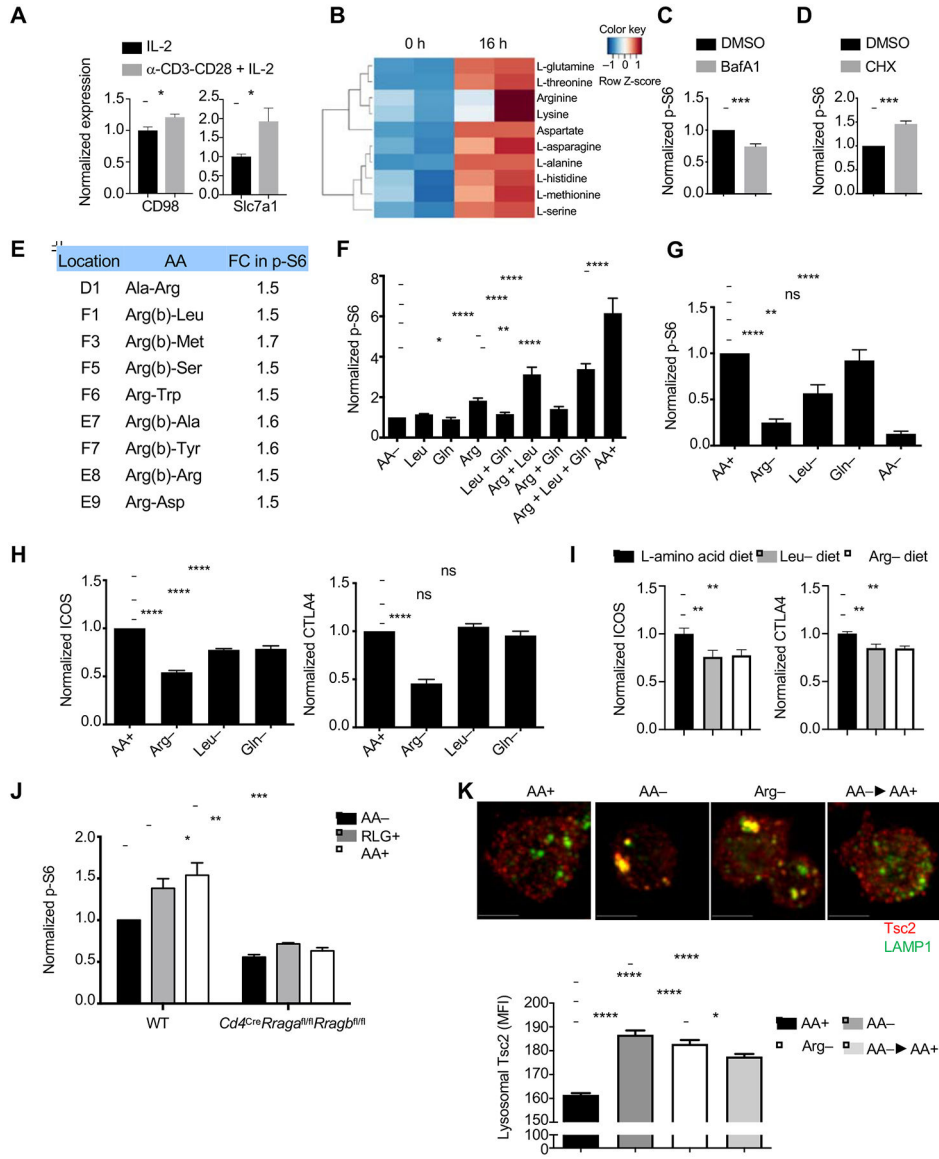
Figure 4. Amino acids maintain mTORC1 activity in aTreg cells

(A) CD98 (n = 3) or Slc7a1 (n = 5) expression on Treg cells stimulated with IL-2 or α-CD3-CD28 mAb plus IL-2 overnight (aTreg cells). (B) Heatmap showing the relative accumulation of amino acids in Treg cells stimulated with or without α-CD3-CD28 mAb. (C and D) p-S6 in aTreg cells rested for 1 h in complete medium in the presence of DMSO, bafilomycin A1 (BafA1) (C), or cycloheximide (CHX) (D) (n = 4). (E) Fold-change (FC) of p-S6 signals upregulated by 1.5-fold or more in aTreg cells cultured in PM-M2 amino acid screening plates for 30 min. (F) p-S6 signals in aTreg cells that were rested in amino-acid free (AA−) medium for 1 h, and then restimulated for 30 min under the indicated conditions. Leu, leucine; Gln, glutamine; Arg, arginine; AA+, full amino acids (n > 6). (G) p-S6 signals in aTreg cells incubated for 1 h with amino acid-sufficient medium (AA+) or medium lacking Arg (Arg−), Leu (Leu−), Gln (Gln−), or all amino acids (AA−). (H) Treg cells were stimulated for three days in AA+, Arg−, Leu−, or Gln− medium. Quantification of the

normalized CTLA4 and ICOS expression (n = 4). (I) Normalized CTLA4 and ICOS expression in Treg cells isolated from mice fed L-amino acid control, arginine-deficient (Arg– diet), or leucine-deficient (Leu– diet) diets (n = 8). (J) Treg cells from WT or $Cd4^{\mathrm{Cre}}Rraga^{\mathrm{fl/fl}}Rragb^{\mathrm{fl/fl}}$ mice were activated to generate aTreg cells, following by resting and restimulation for 30 min under the indicated conditions for quantification of p-S6 signals (n = 2). (K) Imaging analysis of Tsc2 and LAMP1 in aTreg cells incubated with amino acids for 90 min (AA+), without amino acids (AA–) or Arg (Arg–) for 90 min, or starved for amino acids for 60 min followed by amino acid refeeding for 30 min (AA– [barb2right] AA+). Scale bar: 5 mm (n = 2 biological replicates and > 30 cells per condition). Data in graphs represent mean ± SEM. ns, not significant; *p < 0.05; **p < 0.01; ***p < 0.001; ****p < 0.0001; two-tailed Student's t-test (A, C, D) or one-way ANOVA (F– K). Data are representative of one (B, J) or two (A, CD98; E, K), or pooled from two (A, Slc7a1; C, D, G, H), four (I) or five (F) independent experiments. See also Figure S4.
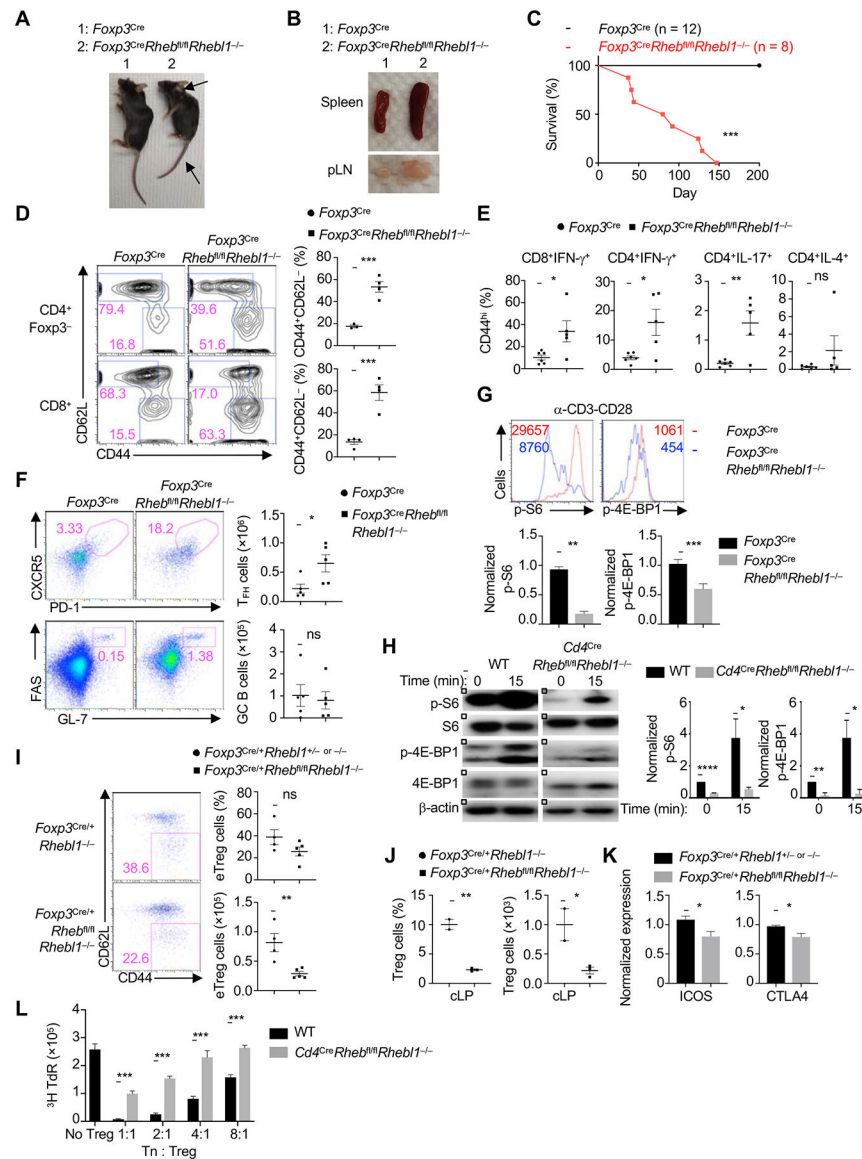
Figure 5. Rheb1/2 deletion disrupts eTreg cell accumulation and function

(A) Image of 1.5-month-old *Foxp3*^Cre or *Foxp3*^Cre*Rheb*^fl/fl*Rhebl1*^−/− mice. Arrows indicate skin inflammation and alopecia. (B) Image of the spleen and peripheral lymph nodes (pLN) from *Foxp3*^Cre or *Foxp3*^Cre*Rheb*^fl/fl*Rhebl1*^−/− mice. (C) Survival of *Foxp3*^Cre or *Foxp3*^Cre*Rheb*^fl/fl*Rhebl1*^−/− mice. (D) FACS analysis of CD44 and CD62L expression on splenic CD4^+Foxp3^− and CD8^+ T cells from *Foxp3*^Cre or *Foxp3*^Cre*Rheb*^fl/fl*Rhebl1*^−/− mice. Right, quantification of the frequencies of CD44^+CD62L^−CD4^+Foxp3^− and CD44^+CD62L ^−CD8^+ T cells in the spleen (n = 4). (E) Quantification of the frequencies of the indicated cytokine-producing CD44^hiCD8^+ and CD44^hiCD4^+Foxp3^− (depicted as CD4^+) T cells in the spleen of *Foxp3*^Cre or *Foxp3*^Cre*Rheb*^fl/fl*Rhebl1*^−/− mice (n ≥ 5). (F) FACS analysis of PD-1^+CXCR5^+ T_FH cells (top) and GL-7^+FAS^+ GC B cells (bottom). Right, Quantification of T_FH and GC B cell numbers (n = 5). (G) Splenic Foxp3-YFP^+ Treg from *Foxp3*^Cre or *Foxp3*^Cre*Rheb*^fl/fl*Rhebl1*^−/− mice were stimulated with α-CD3-CD28 mAb for 4 h. Top,

FACS analysis of p-S6 and p-4E-BP1. Bottom, quantification of p-S6 and p-4E-BP1 signals (n > 4). (H) Immunoblot analysis of phosphorylated and total S6 or 4E-BP1 in Treg cells from WT or $Cd4^{Cre}Rheb^{fl/fl}Rhebl1^{-/-}$ mice after stimulation with α-CD3-CD28 mAb crosslinking for the indicated times. The space indicates removal of irrelevant lanes. Right, quantification of p-S6 and p-4E-BP1 normalized to β-actin (n = 4). (I) FACS analysis of CD44 versus CD62L expression on splenic Foxp3-YFP$^+$ Treg cells from $Foxp3^{Cre/+}Rhebl1^{+/- \text{ or } -/-}$ or $Foxp3^{Cre/+}Rheb^{fl/fl}Rhebl1^{-/-}$ mice. Right, quantification of the numbers of splenic CD44^{hi}CD62L^{lo} eTreg cells (n   4). (J) Quantification of the frequency and number of Foxp3-YFP$^+$ Treg cells in the colon lamina propria (cLP) of $Foxp3^{Cre/+}Rhebl1^{-/-}$ or $Foxp3^{Cre/+}Rheb^{fl/fl}Rhebl1^{-/-}$ mice (n   2). (K) Quantification of ICOS and CTLA4 expression in splenic Foxp3-YFP$^+$ Treg cells from $Foxp3^{Cre/+}Rhebl1^{+/- \text{ or } -/-}$ or $Foxp3^{Cre/+}Rheb^{fl/fl}Rhebl1^{-/-}$ mice (n > 4). (L) Suppressive activity of Treg cells from WT or $Cd4^{Cre}Rheb^{fl/fl}Rhebl1^{-/-}$ mice (n = 6). Numbers on plots are the frequency of cells in indicated gates. Numbers in histograms show the mean fluorescence intensity. Data in graphs represent mean ± SEM. ns, not significant; *p < 0.05; **p < 0.01; ***p < 0.001; two-tailed Student's t-test. Data are representative of one (H, L) or more than four (A, B), or pooled from one (J), two (I, K), three (D, G) or four (E, F) independent experiments. See also Figure S5.
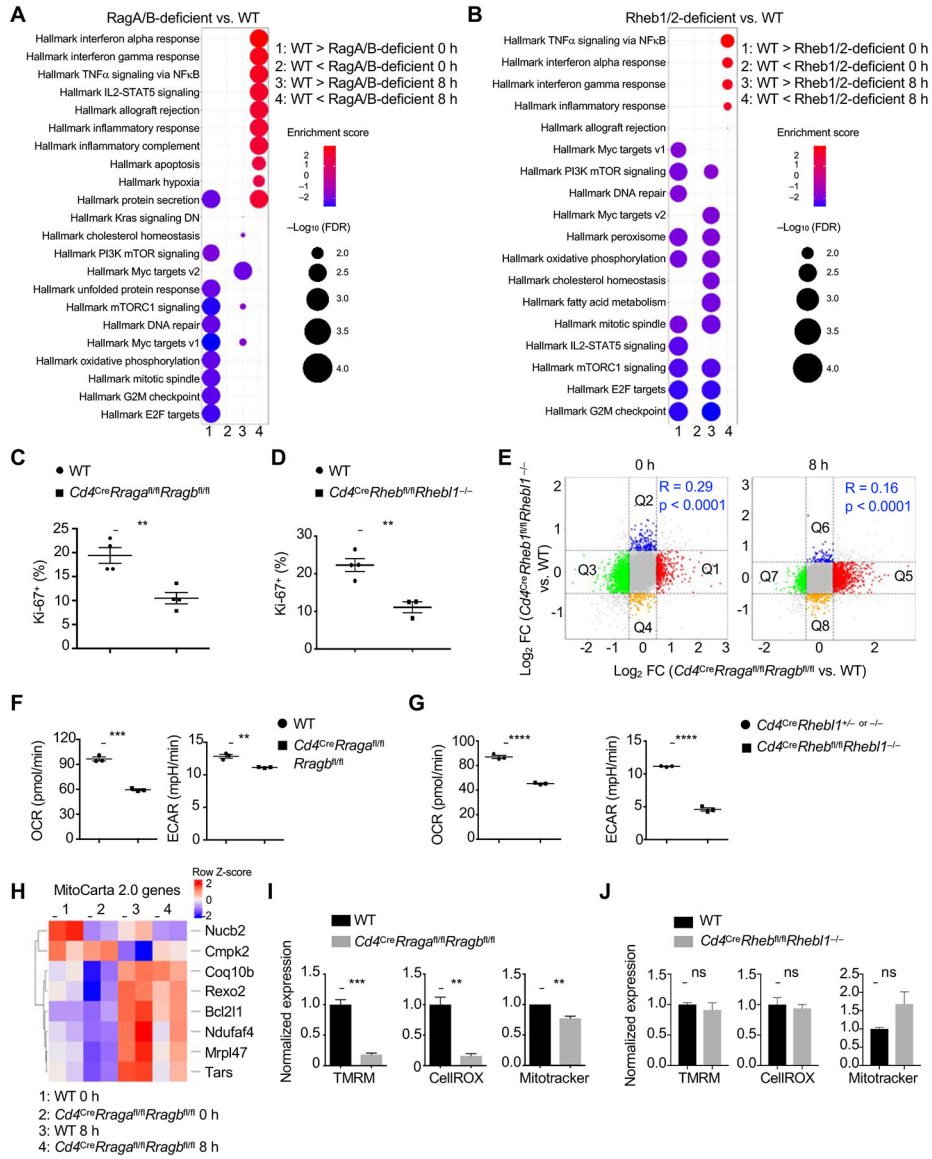
Figure 6. Regulation of transcriptional and metabolic programs by RagA/B and Rheb1/2

(A and B) Treg cells from WT or $Cd4$^Cre$Rraga$^fl/fl$Rragb$^fl/fl (A) and WT or $Cd4$^Cre$Rheb$^fl/fl$Rhebl1$^−/− mice (B) were stimulated with α-CD3-CD28 mAb for 0 or 8 h. Gene set enrichment analysis identified upregulated (red) and downregulated (blue) Hallmark pathways in RagA/B-deficient Treg cells (A) or Rheb1/2-deficient Treg cells (B), as shown on bubble plots. (C and D) Quantification of the frequency of splenic Ki-67^{+} Treg cells from WT or $Cd4$^Cre$Rraga$^fl/fl$Rragb$^fl/fl (C; n = 4) or WT or $Cd4$^Cre$Rheb$^fl/fl$Rhebl1$^−/− mice (D; n 3). (E) Fold-change (FC) versus FC plot analysis of genes expressed by RagA/B-deficient Treg cells with Rheb1/2-deficient Treg cells (versus WT controls in each case) at 0 h (left) and 8 h (right). R, Pearson's correlation coefficient. Colors indicate regions where genes are only differentially-expressed (DE) in RagA/B- or Rheb1/2-deficient Treg cells. (F and G) Treg cells from WT or $Cd4$^Cre$Rraga$^fl/fl$Rragb$^fl/fl mice (F) or WT or $Cd4$^Cre$Rheb$^fl/fl$Rhebl1$^−/− mice (G) were stimulated with α-CD3-CD28 mAb for 16 h,

followed by Seahorse metabolic flux analysis of mitochondrial oxygen consumption rate (OCR) and extracellular acidification rate (ECAR) (n = 3). (H) Heatmap showing DE mitochondrial genes in WT or RagA/B-deficient Treg cells at 0 and 8 h. (I) Quantification of TMRM, CellROX, and Mitotracker in splenic Treg cells from WT or $Cd4^{\text{Cre}}Rraga^{\text{fl/fl}}Rragb^{\text{fl/fl}}$ mice (n = 6 for TMRM and CellROS; n = 3 for Mitotracker). (J) Quantification of TMRM, CellROX, and Mitotracker in splenic Treg cells from WT or $Cd4^{\text{Cre}}Rheb^{\text{fl/fl}}Rhebl1^{-/-}$ mice (n = 3). Data in graphs represent mean ± SEM. ns, not significant; **p < 0.01; ***p < 0.001; two-tailed Student's t-test. Data are representative of one (A, B, E, H, I, Mitotracker; J) or three (F, G), or pooled from three (C, D, I, TMRM and CellROX) independent experiments. See also Figure S6.
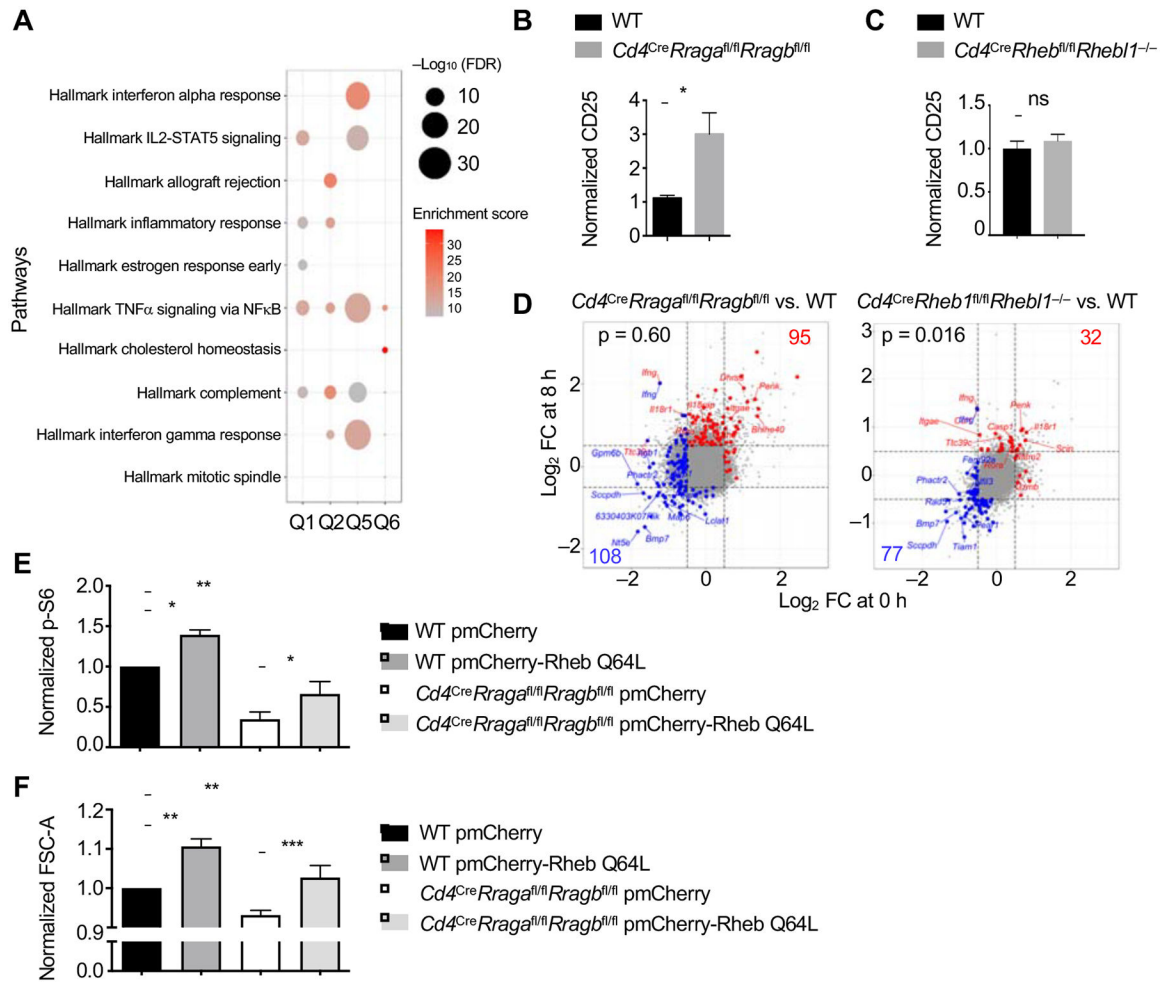
Figure 7. eTreg cell signatures are differentially regulated by RagA/B and Rheb1/2
(A) Functional enrichment of Hallmark pathways in genes upregulated in the absence of RagA/B or Rheb1/2 at 0 or 8 h, as shown on bubble plots. (B and C) Quantification of CD25 expression on Treg cells from WT or $Cd4^{Cre}Rraga^{fl/fl}Rragb^{fl/fl}$ mice (B; n = 5), or WT or $Cd4^{Cre}Rheb^{fl/fl}Rhebl1^{-/-}$ mice (C; n > 4). (D) Fold-change (FC) versus FC plot analysis (x-axis, 0 h; y-axis, 8 h) of genes expressed by RagA/B-deficient Treg cells versus WT (left), or Rheb1/2-deficient Treg cells versus WT (right). The blue dots show downregulated and the red dots show upregulated eTreg cell signature genes. The numbers show differentially-expressed genes. The p-value indicates enrichment for eTreg cell signature genes. (E and F) WT and RagA/B-deficient Treg cells were transduced with indicated vectors and stimulated with α-CD3-CD28 mAb for 3 h for quantification of p-S6 (E) or FSC-A (F) in pmCherry+ Treg cells transduced with the indicated vectors (n = 6). Data in graphs represent mean ± SEM. ns, not significant; *p < 0.05; **p < 0.01; ***p < 0.001; two-tailed Student's t-test (B, C) or one-way ANOVA (E, F). Data are representative of one (A, D), or pooled from two (F) or three (B, C, E) independent experiments. See also Figure S7.